

Through Vial Impedance Spectroscopy (TVIS) *Dual-electrode System for Process Parameter Determination*

Geoff Smith

Leicester School of Pharmacy, De Montfort University, United Kingdom

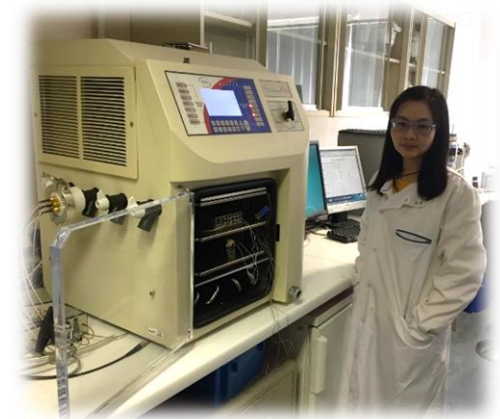
ISL-FD Midwest Chapter Annual Meeting, April 12th 2018
Midwest Conference Centre, Northlake, IL 60164, USA

Through Vial Impedance Spectroscopy



Outline

- Description of TVIS measurement system
- TVIS dielectric loss mechanisms
- First time report on the use of dual-electrode system and its applications
 - Ice region specific temperature prediction (T_i, T_b)
 - Drying rate determination
 - Heat transfer coefficient (K_v) determination
- Acknowledgements



Through Vial Impedance Spectroscopy (TVIS)

Description of Measurement System

Introduction to the TVIS System

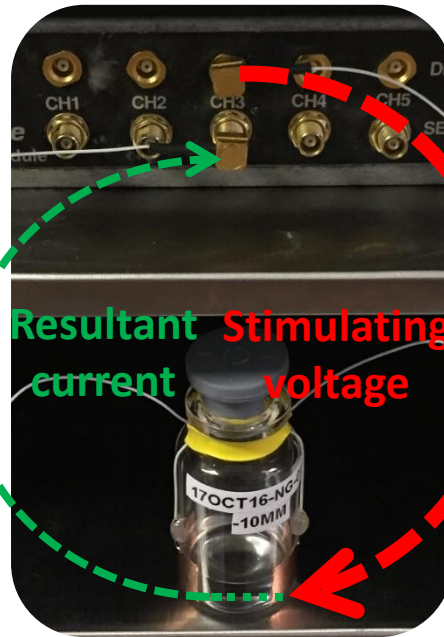
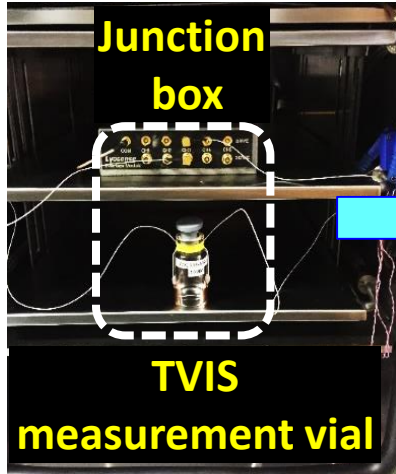
- Impedance spectroscopy characterizes the ability of materials to conduct electricity under an applied an oscillating voltage (of varying frequency)
- Impedance measurements **across a vial** rather than **within the vial**
- Hence **“Through Vial Impedance Spectroscopy”**
- Features
 - Single vial “non-product invasive”
 - Both freezing and drying characterised in a single technique
 - Non-perturbing to the packing of vials
 - Stopper mechanism unaffected



SV product temperature	
SV sublimation rate	
SV end point	



Freeze drying chamber



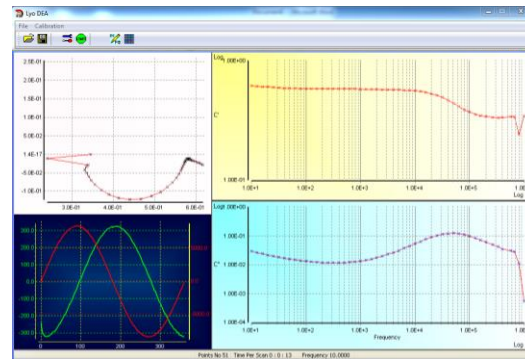
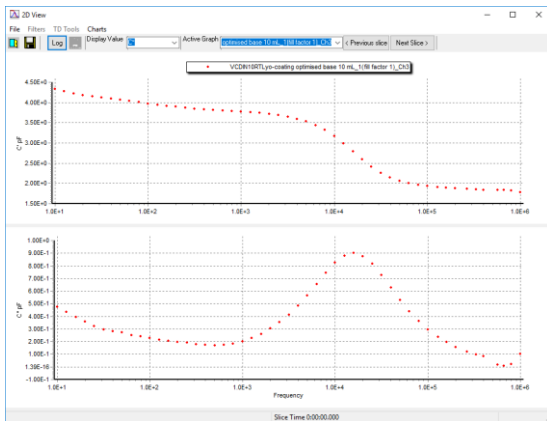
Pass-through



LyoView™ analysis software

LyoDEA™ measurement software

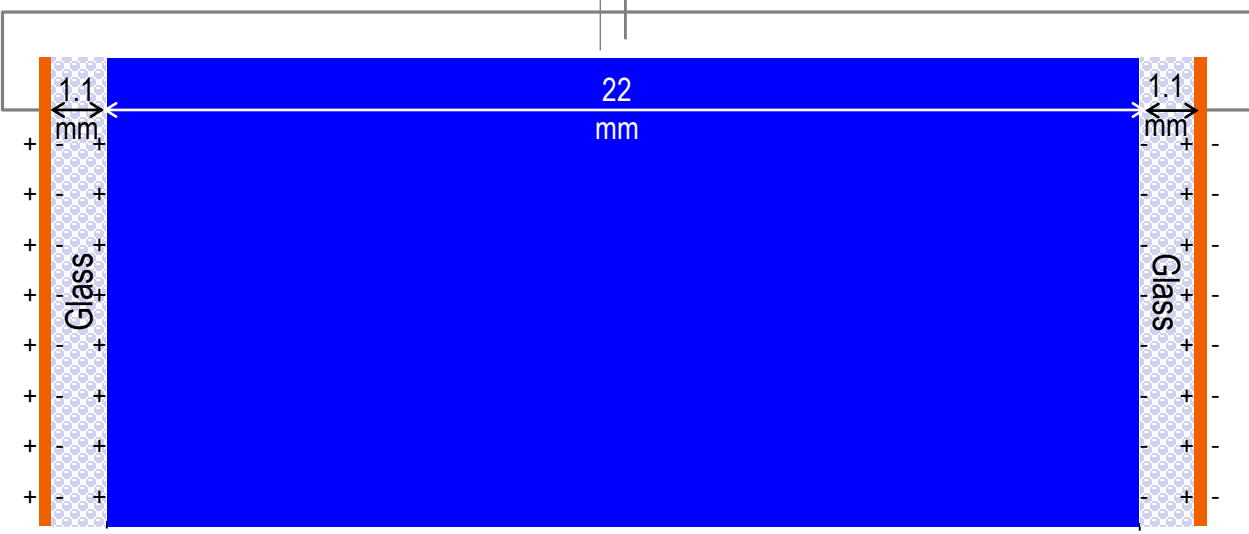
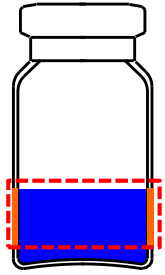
TVIS system (I to V convertor)



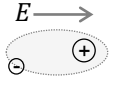
Through Vial Impedance Spectroscopy (TVIS)

Dielectric Loss Mechanisms

Measurement vial



Electronic polarization
distortion of electrons
relative to the nuclei

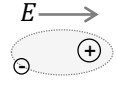


Atomic polarization
distortion of nuclei across
a heteroatom bond by
stretching and bending



**Instantaneous polarization dominant
mechanism in the glass wall**

Electronic polarization
distortion of electrons
relative to the nuclei



Atomic polarization
distortion of nuclei across
a heteroatom bond by
stretching and bending

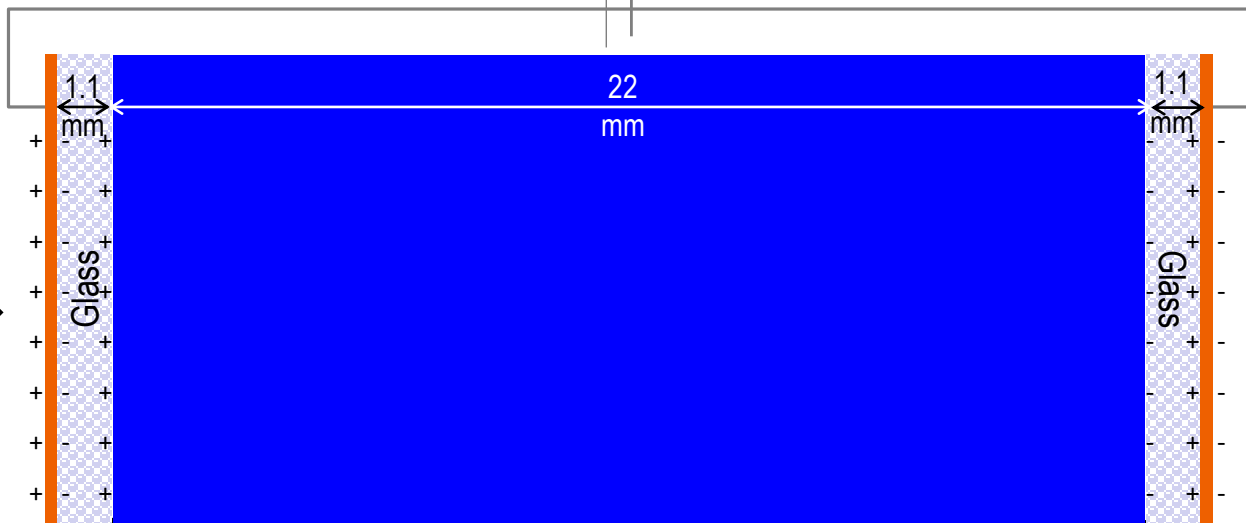
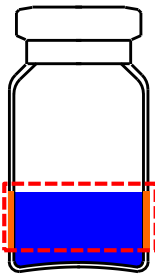


**Instantaneous polarization dominant
mechanism in the glass wall**

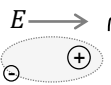
TVIS response for empty vial

TVIS response for empty vial

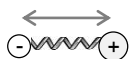
Measurement vial



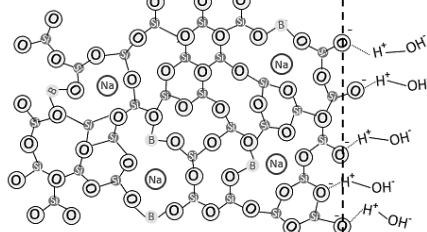
Electronic polarization
distortion of electrons
relative to the nuclei



Atomic polarization
distortion of nuclei across
a heteroatom bond by
stretching and bending



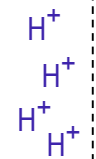
**Instantaneous polarization dominant
mechanism in the glass wall**



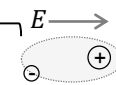
**Space charge polarization
(weak frequency dependence)**

TVIS response for empty vial

MW (space-charge) polarization at glass wall – sample interface



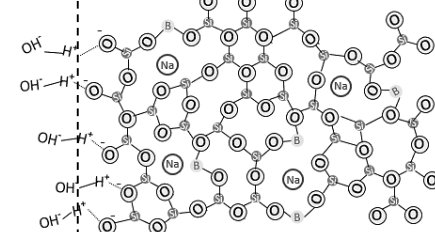
Electronic polarization
distortion of electrons
relative to the nuclei



Atomic polarization
distortion of nuclei across
a heteroatom bond by
stretching and bending



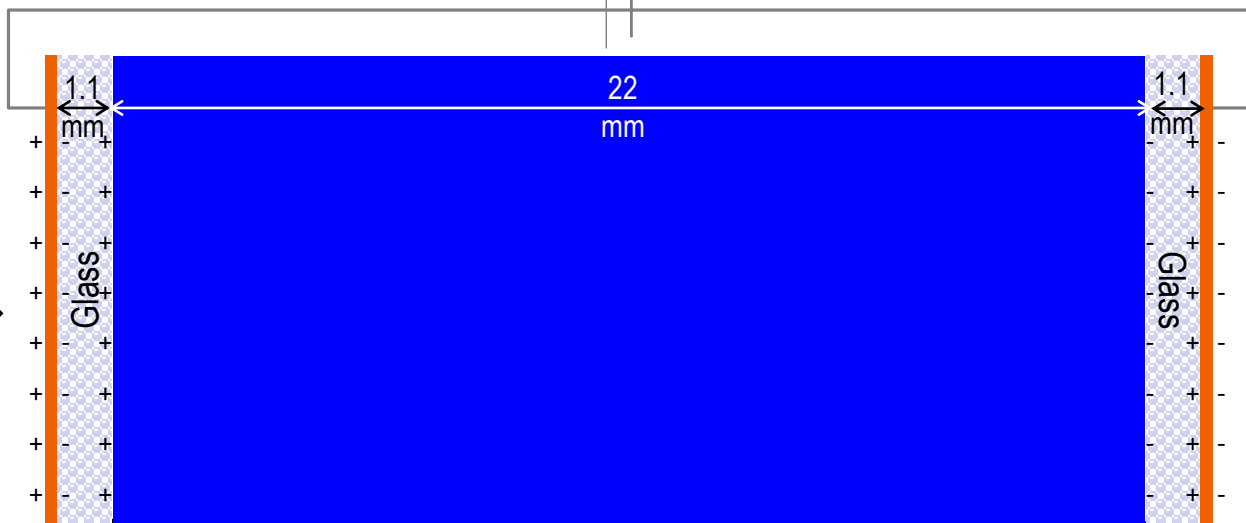
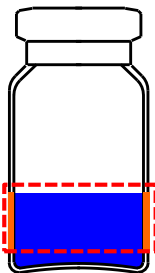
**Instantaneous polarization dominant
mechanism in the glass wall**



**Space charge polarization
(weak frequency dependence)**

TVIS response for empty vial

Measurement vial



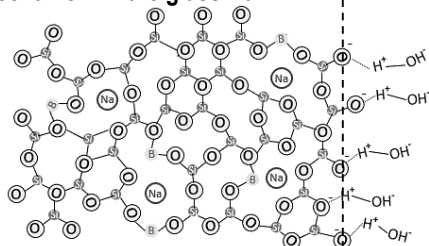
Electronic polarization
distortion of electrons
relative to the nuclei



Atomic polarization
distortion of nuclei across
a heteroatom bond by
stretching and bending



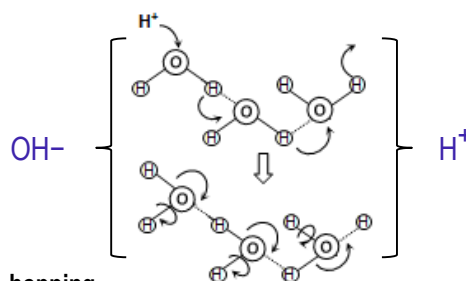
**Instantaneous polarization dominant
mechanism in the glass wall**



**Space charge polarization
(weak frequency dependence)**

**MW (space-charge) polarization at glass
wall – sample interface**

TVIS response for empty vial



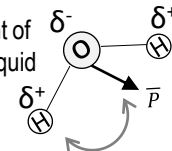
Proton-hopping

Conduction of protons in liquid water occurs
through the Grotthuss "hop-turn" mechanism

Conductivity in pure water

Dipolar polarization

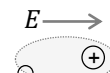
re-orientation/alignment of
permanent dipoles in liquid
water (Debye-like
relaxation)



**Polarization mechanisms in liquid water
(relaxation time, $\tau \sim 9$ ps at 20°C)**

TVIS response for liquid water

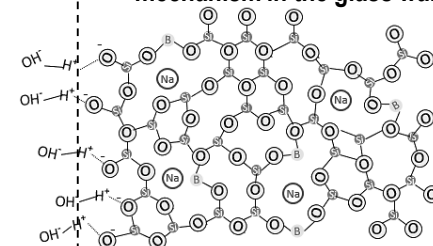
Electronic polarization
distortion of electrons
relative to the nuclei



Atomic polarization
distortion of nuclei across
a heteroatom bond by
stretching and bending



**Instantaneous polarization dominant
mechanism in the glass wall**

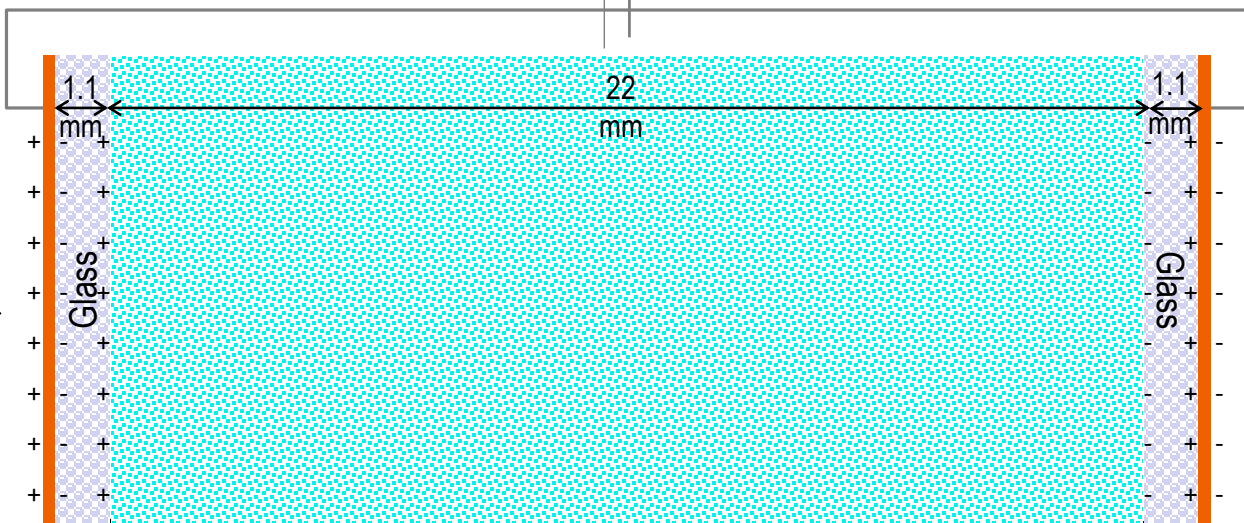
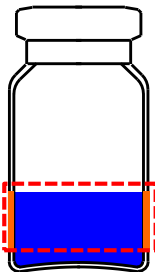


**Space charge polarization
(weak frequency dependence)**

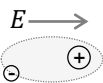
**MW (space-charge) polarization at glass
wall – sample interface**

TVIS response for empty vial

Measurement vial



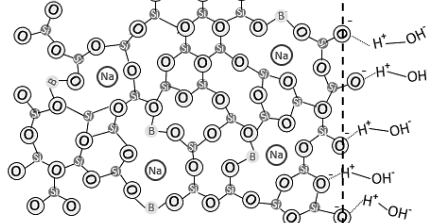
Electronic polarization
distortion of electrons relative to the nuclei



Atomic polarization
distortion of nuclei across a heteroatom bond by stretching and bending



Instantaneous polarization dominant mechanism in the glass wall

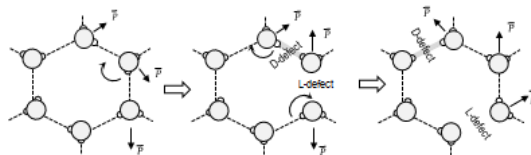


Space charge polarization
(weak frequency dependence)

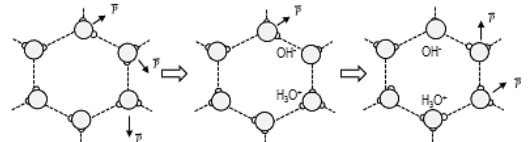
MW (space-charge) polarization at glass wall – sample interface

TVIS response for empty vial

Dominant at $T > 235$ K (approx. -40 °C)
Generation/migration of L- and D- orientation defects in ice Ih



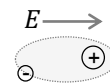
Dominant at $T < 235$ K (approx. -40 °C)
Generation/migration of H_3O^+/OH^- ion pairs (ionic defects) in ice Ih (similar to the Grotthus mechanism)



Polarization mechanism in ice

TVIS response for frozen water (ice)

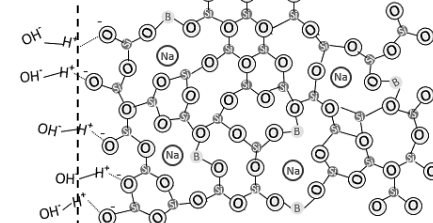
Electronic polarization
distortion of electrons relative to the nuclei



Atomic polarization
distortion of nuclei across a heteroatom bond by stretching and bending



Instantaneous polarization dominant mechanism in the glass wall



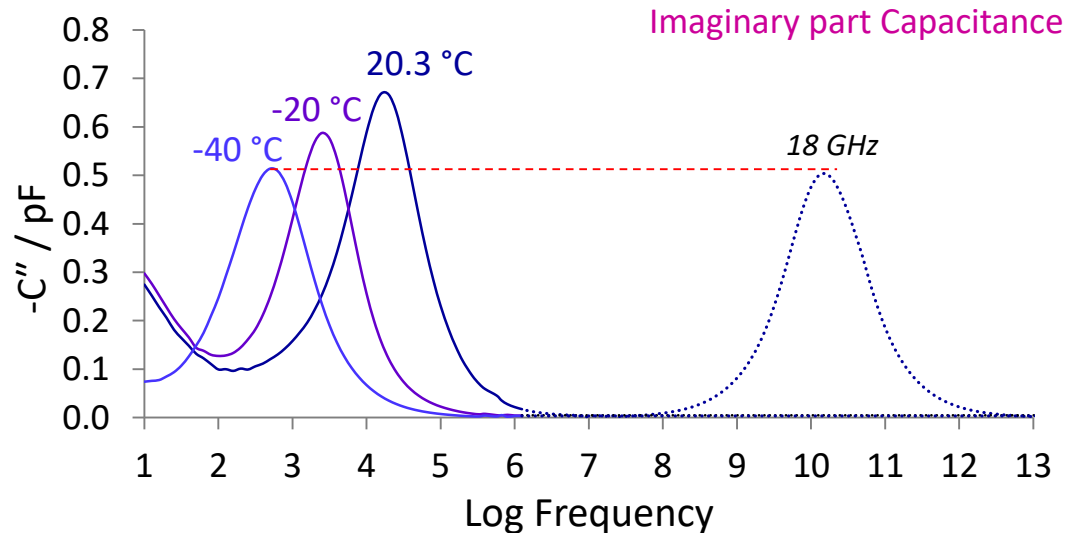
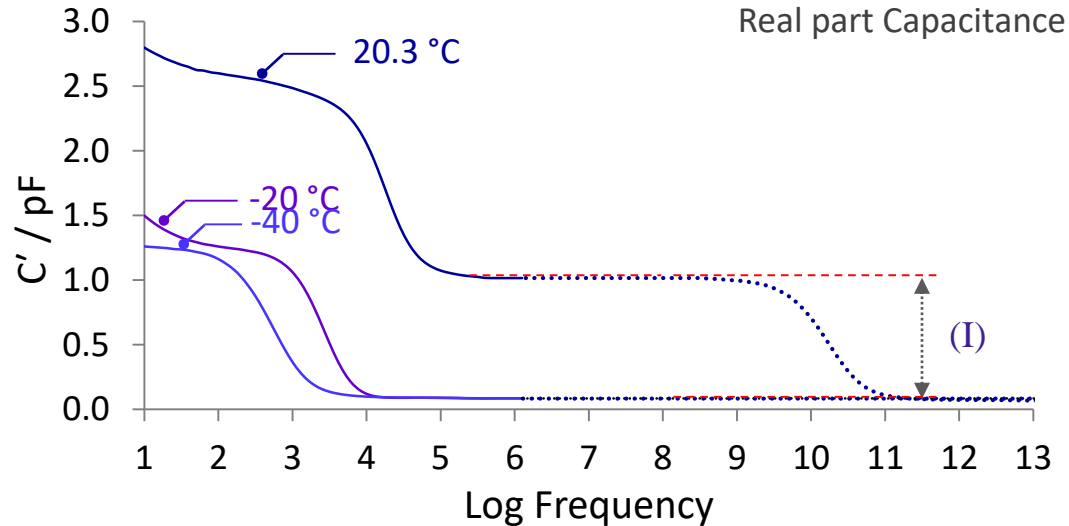
Space charge polarization
(weak frequency dependence)

MW (space-charge) polarization at glass wall – sample interface

TVIS response for empty vial

Frozen Water and Dielectric Relaxation of Ice

I. : The polarization of the water dipole in liquid water at 20 °C, with a dielectric loss peak frequency of ~ 18 GHz

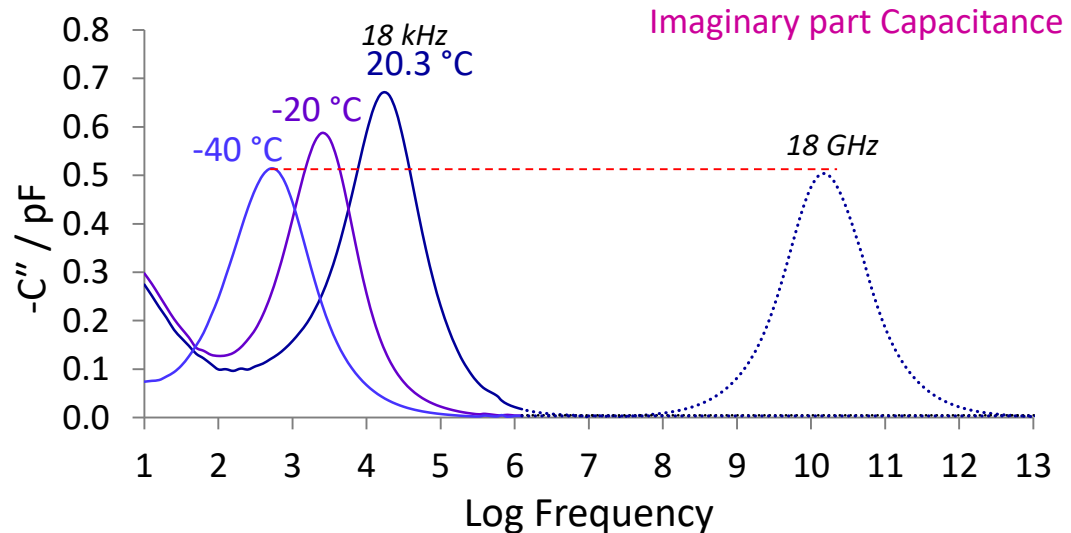
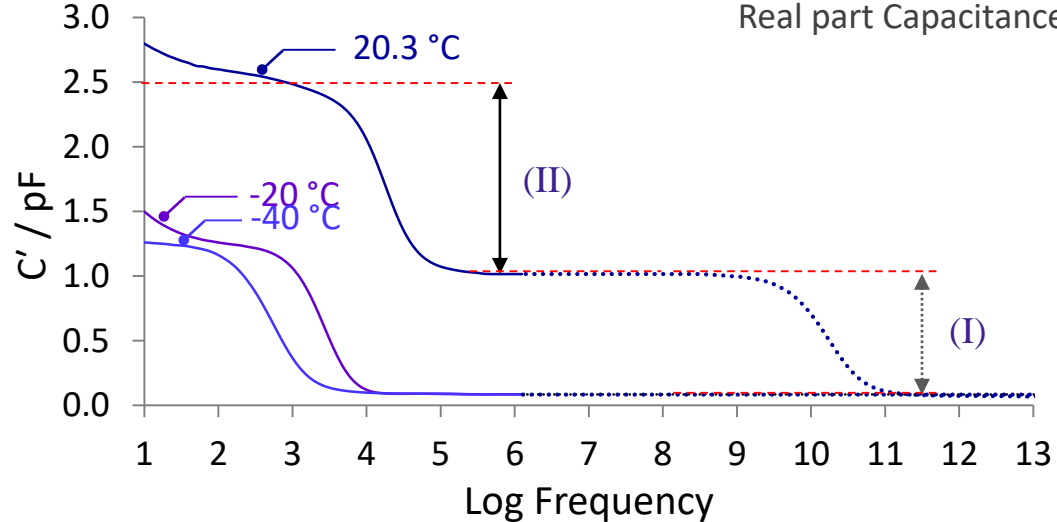


Frozen Water and Dielectric Relaxation of Ice



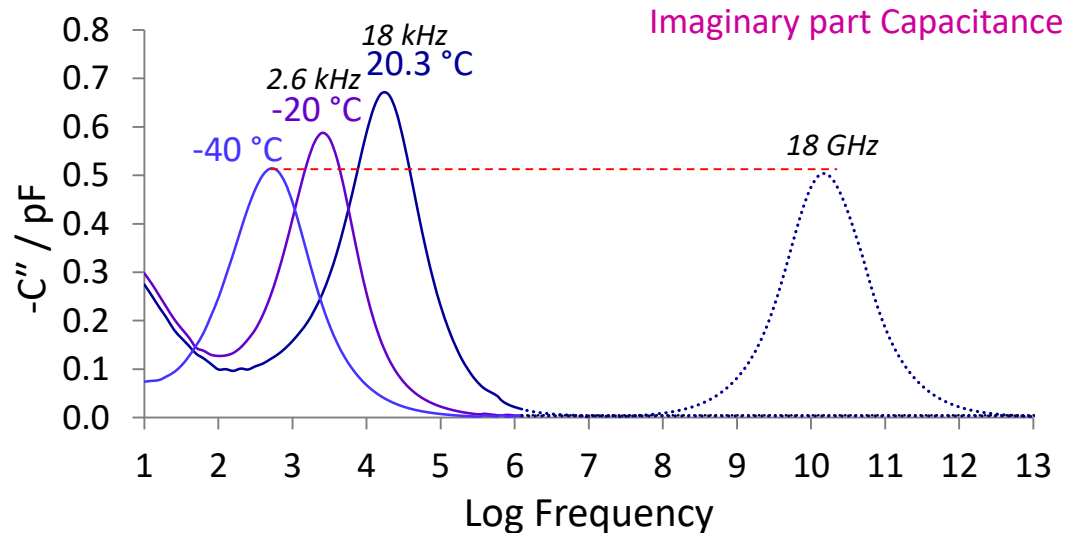
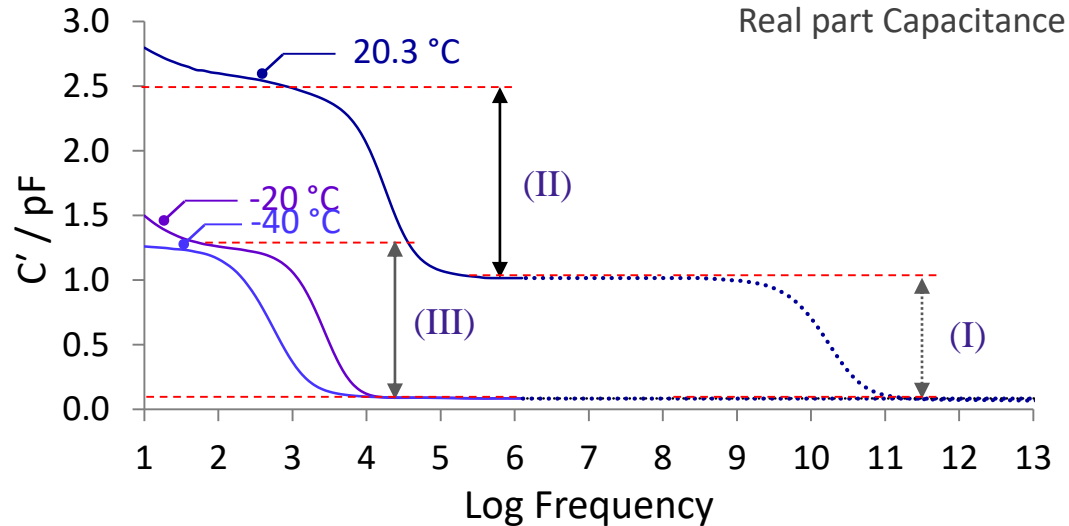
Real part Capacitance

- I. : The polarization of the water dipole in liquid water at 20 °C, with a dielectric loss peak frequency of ~ 18 GHz
- II. : The Maxwell-Wagner (MW) polarization of the glass wall of the TVIS vial at 20 °C, with a dielectric loss peak frequency of 17.8 kHz



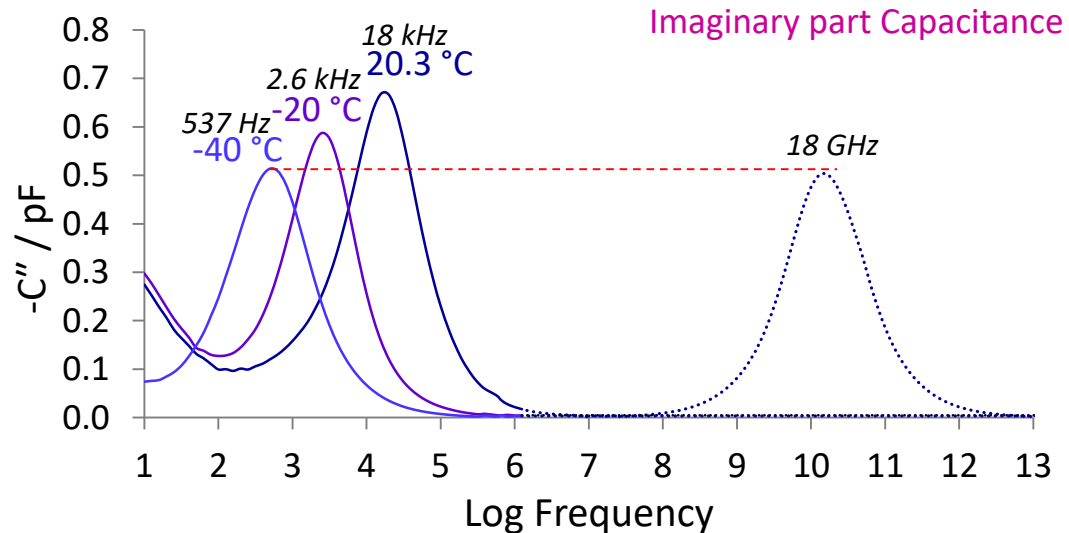
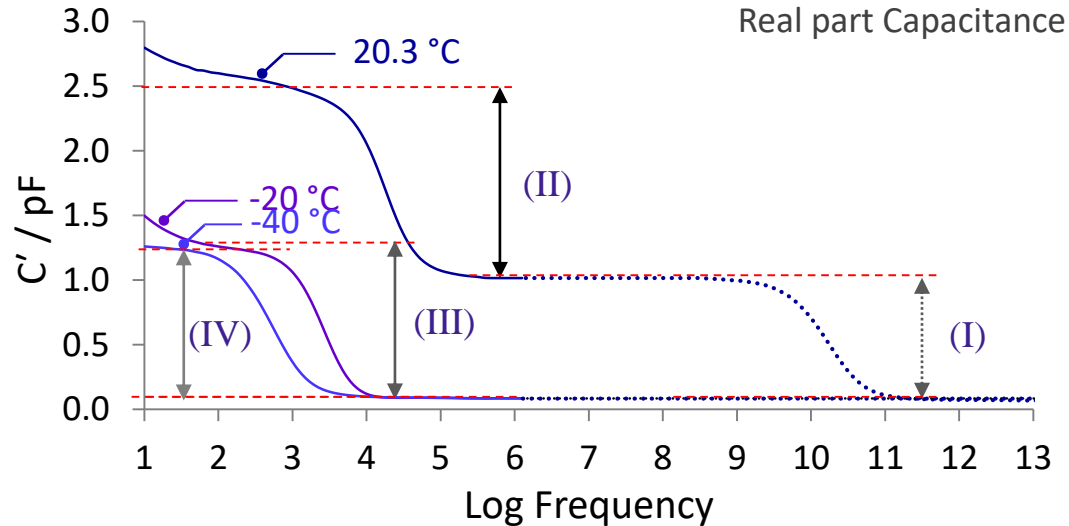
Frozen Water and Dielectric Relaxation of Ice

- I. : The polarization of the water dipole in liquid water at 20 °C, with a dielectric loss peak frequency of ~ 18 GHz
- II. : The Maxwell-Wagner (MW) polarization of the glass wall of the TVIS vial at 20 °C, with a dielectric loss peak frequency of 17.8 kHz
- III. : The dielectric polarization of ice at -20 °C, with a dielectric loss peak frequencies of 2.57 kHz



Frozen Water and Dielectric Relaxation of Ice

- I. : The polarization of the water dipole in liquid water at 20 °C, with a dielectric loss peak frequency of ~ 18 GHz
- II. : The Maxwell-Wagner (MW) polarization of the glass wall of the TVIS vial at 20 °C, with a dielectric loss peak frequency of 17.8 kHz
- III. : The dielectric polarization of ice at -20 °C, with a dielectric loss peak frequencies of 2.57 kHz
- IV. : The dielectric polarization of ice at -40 °C with a dielectric loss peak frequencies of 537 Hz.



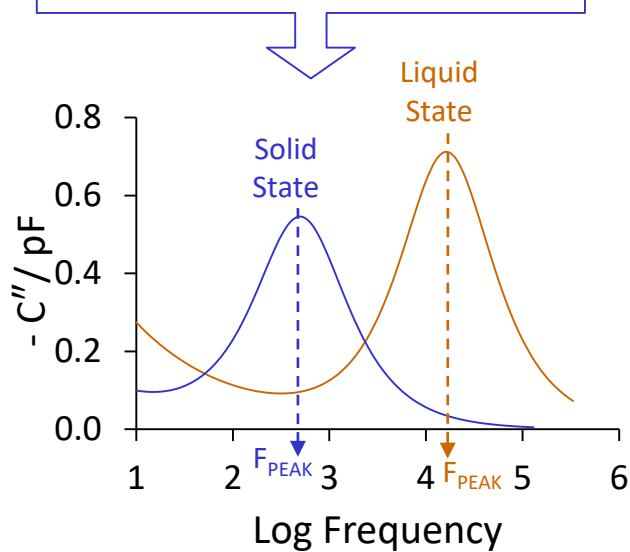
Through Vial Impedance Spectroscopy (TVIS)

Applications

Through Vial Impedance Spectroscopy (TVIS)



Monitoring **Phase Behaviour**
(ice nucleation temperature
and solidification end points
by using F_{PEAK})

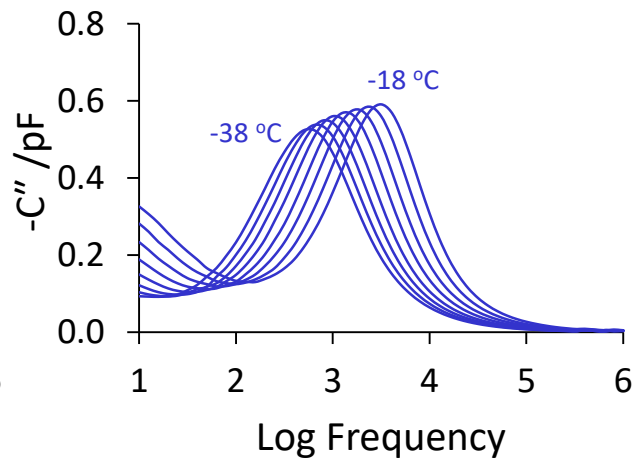
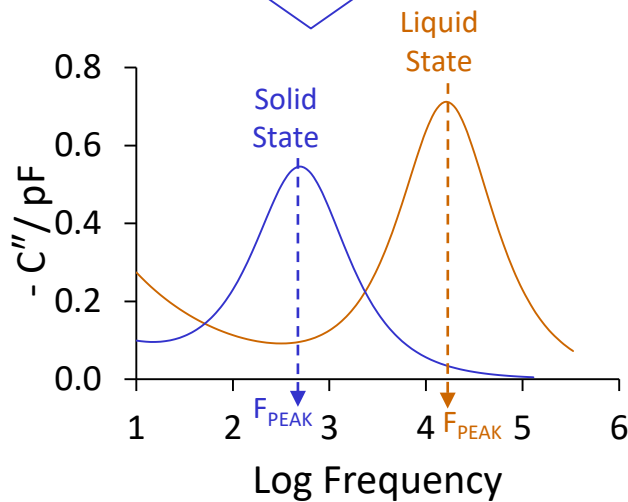


Through Vial Impedance Spectroscopy (TVIS)



Monitoring **Phase Behaviour**
(ice nucleation temperature
and solidification end points
by using F_{PEAK})

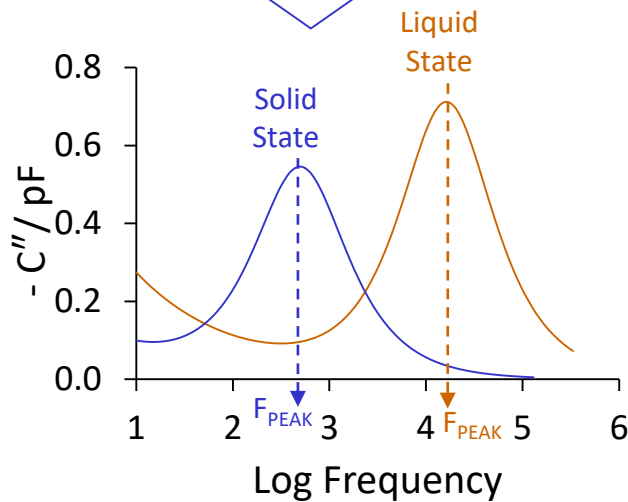
F_{PEAK} temperature calibration
for **predicting temperature** of
the product in primary drying



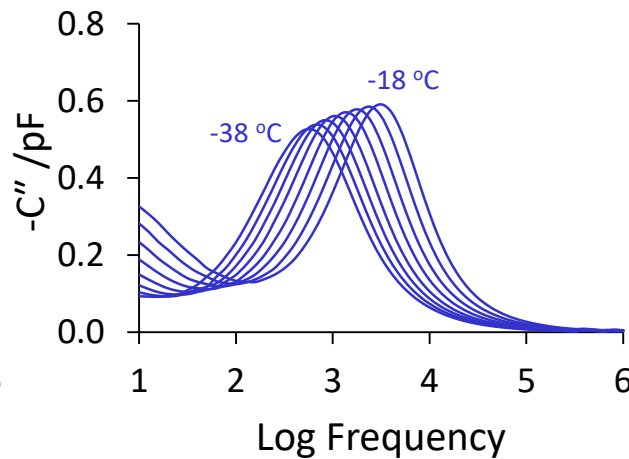
Through Vial Impedance Spectroscopy (TVIS)



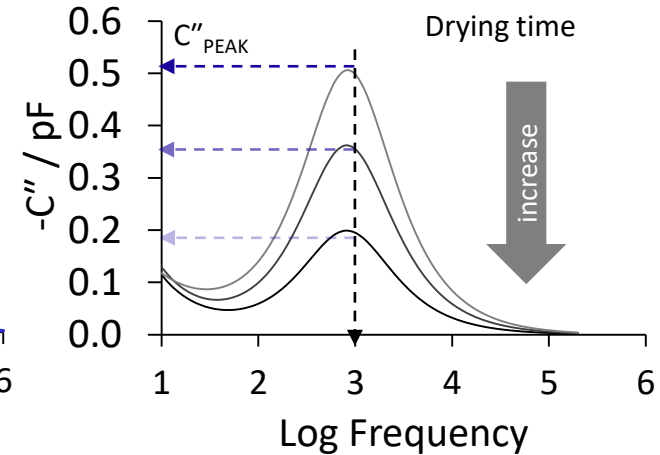
Monitoring **Phase Behaviour**
(ice nucleation temperature
and solidification end points
by using F_{PEAK})



F_{PEAK} temperature calibration
for **predicting temperature** of
the product in primary drying



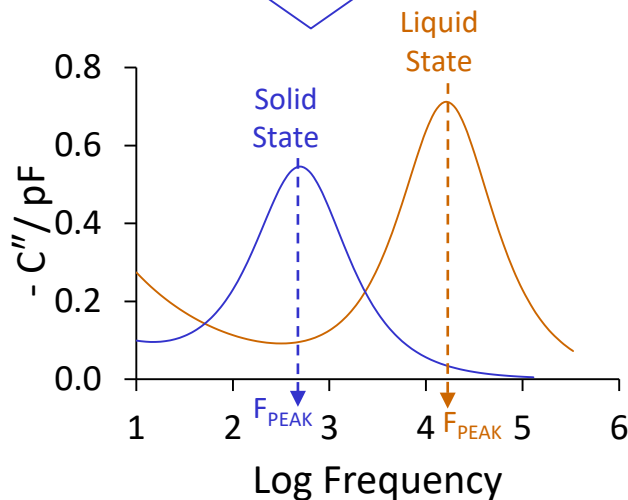
Surrogate **drying rate**
(from $\frac{dC''_{PEAK}}{dt}$)



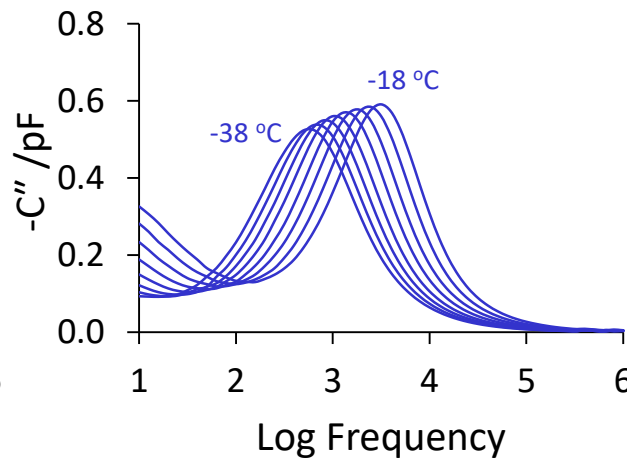
Through Vial Impedance Spectroscopy (TVIS)



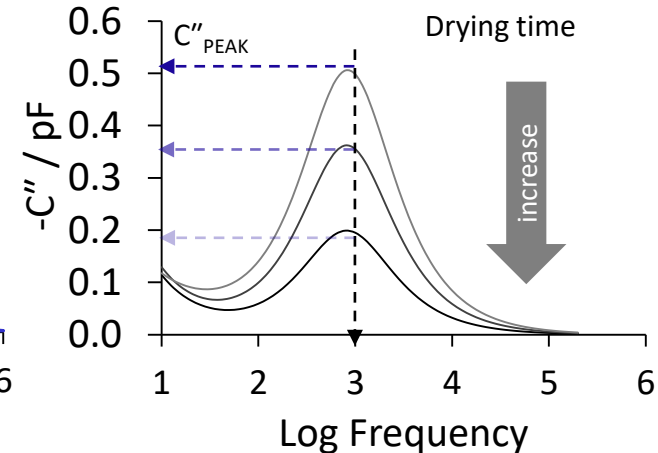
Monitoring **Phase Behaviour**
(ice nucleation temperature
and solidification end points
by using F_{PEAK})



F_{PEAK} temperature calibration
for **predicting temperature** of
the product in primary drying



Surrogate **drying rate**
(from $\frac{dC''_{PEAK}}{dt}$)



C' (~ 100 kHz) is highly sensitive to low ice volumes; therefore it could be used for determination **end point** of primary drying

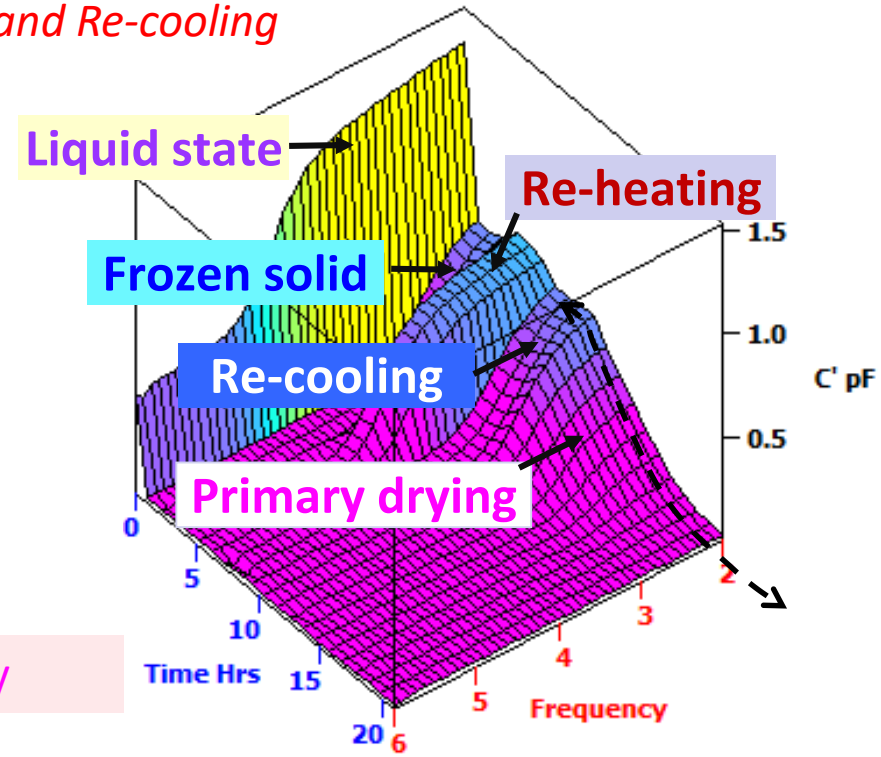
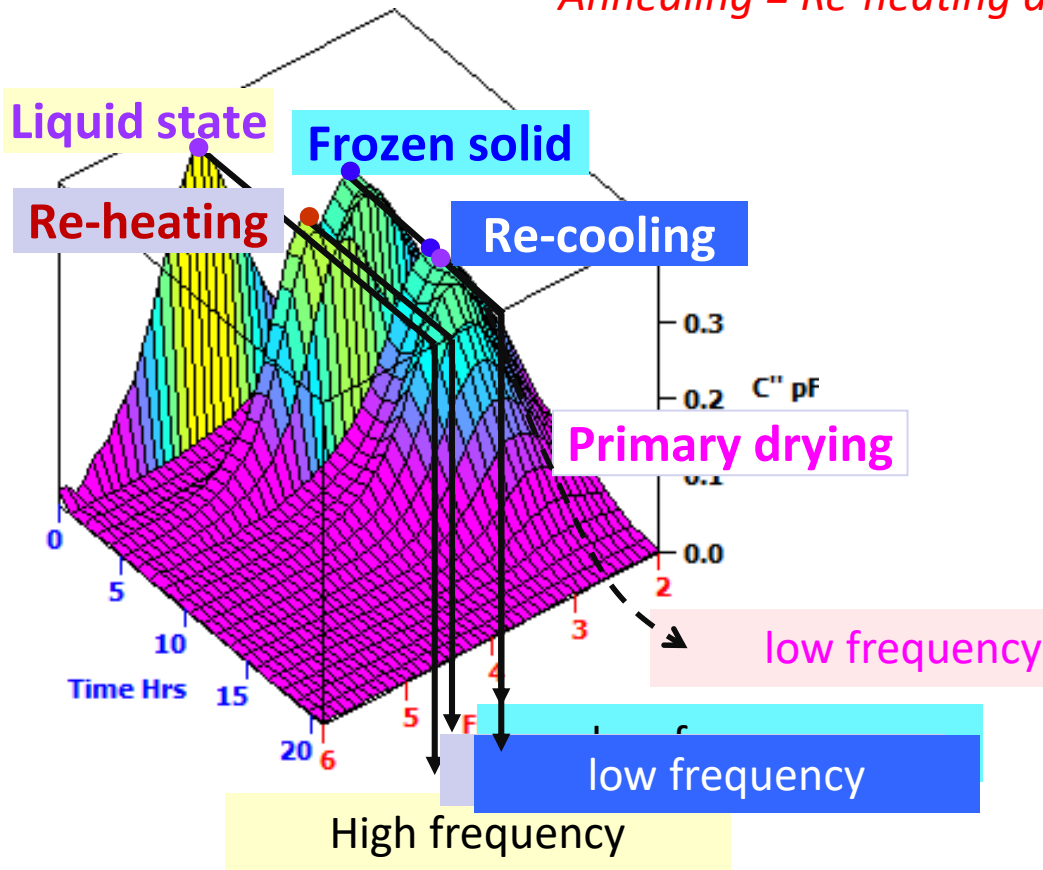
TVIS Response Surface (3D-Plot)



Imaginary Part of Capacitance

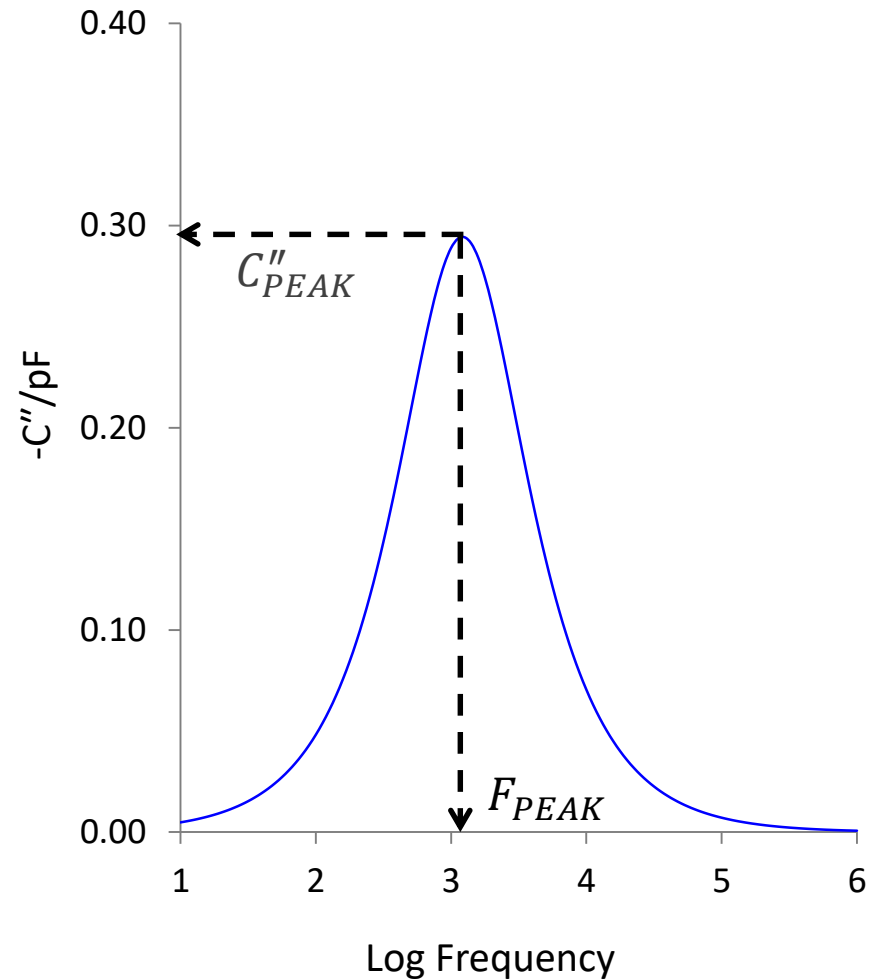
Real Part of Capacitance

Annealing = Re-heating and Re-cooling



Dielectric loss spectrum

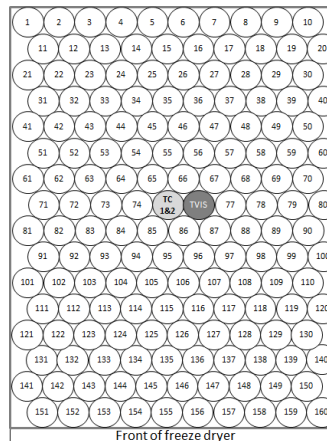
- Data analysing software (*LyoView™*) identifies the peak frequency (F_{PEAK}) and peak amplitude (C''_{PEAK}) in the imaginary part of the capacitance spectrum



Through Vial Impedance Spectroscopy (TVIS)

Dual-electrode system and its applications

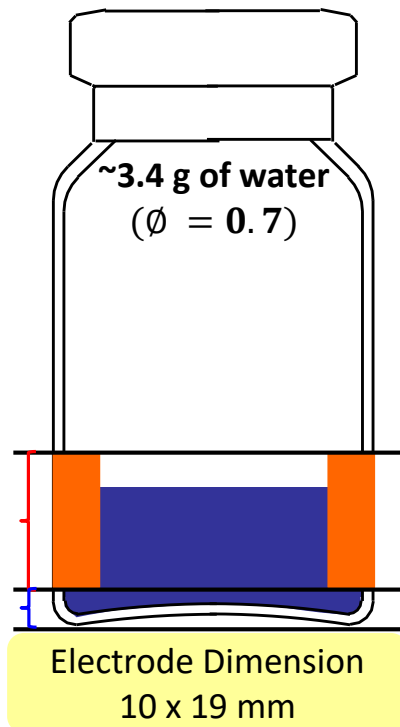
(Ice temperature, Drying rate and Heat transfer coefficient)



Dual-electrode system

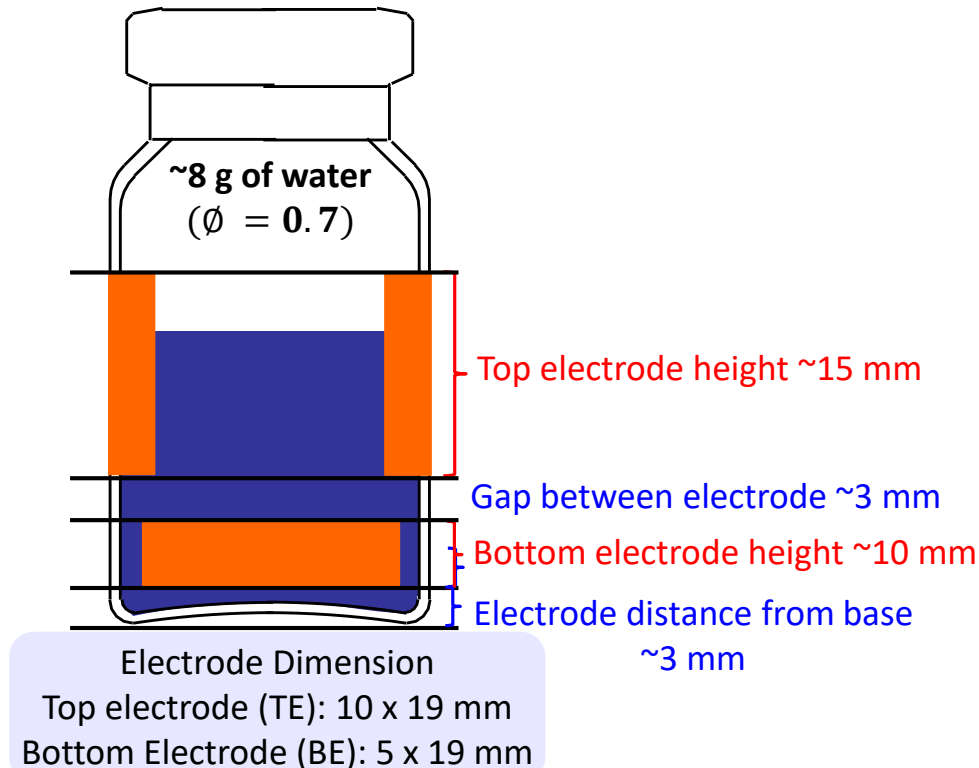
Standard TVIS vial

(Single electrode system)



New feature of TVIS vial

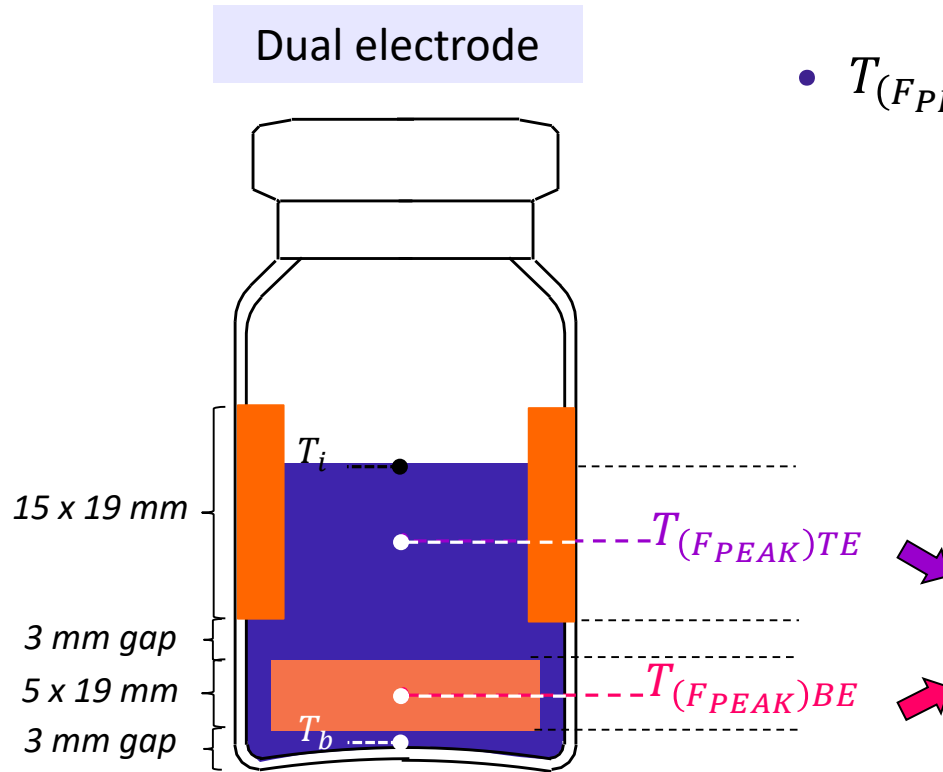
(Dual electrode system)



- A dual electrode system comprises two pairs of copper electrode glued to the external surface of a Type I tubular glass vial.
- This option is suitable for large volume samples, including those used for K_v determination.

Temperature Determination

- $T_{(F_{PEAK})TE}$: TVIS predicted temperature from top electrode (TE)
- $T_{(F_{PEAK})BE}$: TVIS predicted temperature from bottom electrode (BE)



Both T_i and T_b can be estimated by extrapolating from the temperatures predicted from the centers of top electrode ($T_{(F_{PEAK})TE}$) and bottom electrode ($T_{(F_{PEAK})BE}$).

Aims & Objectives

Aims

To determine the heat transfer coefficient (K_v) by using a novel dual electrode TVIS approach

I Temperature calibration of $\log F_{PEAK}$ of top electrode ($T_{(F_{PEAK})TE}$) and bottom electrode ($T_{(F_{PEAK})BE}$)

II Prediction ice temperatures for both electrodes during primary drying

III Temperature calibration of C''_{PEAK}

IV Compensation of C''_{PEAK} during primary drying

V Calibration of C''_{PEAK} for ice layer height

VI Estimation of ice layer height during primary drying

VII Prediction ice temperatures at (i) sublimation interface (T_i) and (ii) vial's base (T_b) including qualification TVIS technique ($T_i = T_{(P_i=P_c)}$)

VIII Comparison of TVIS drying rate ($\Delta m/\Delta t$) with gravimetric method (weight loss)

IX Determination (i) the drying rate ($\Delta m/\Delta t$) and (ii) ice base temperature (T_b) during the steady state period

X Heat transfer coefficient (K_v) calculation

Objective

I

Temperature calibration of $\log F_{PEAK}$ of top electrode ($T_{(F_{PEAK})TE}$) and bottom electrode ($T_{(F_{PEAK})BE}$)

Annealing the sample

In-line TVIS measurement

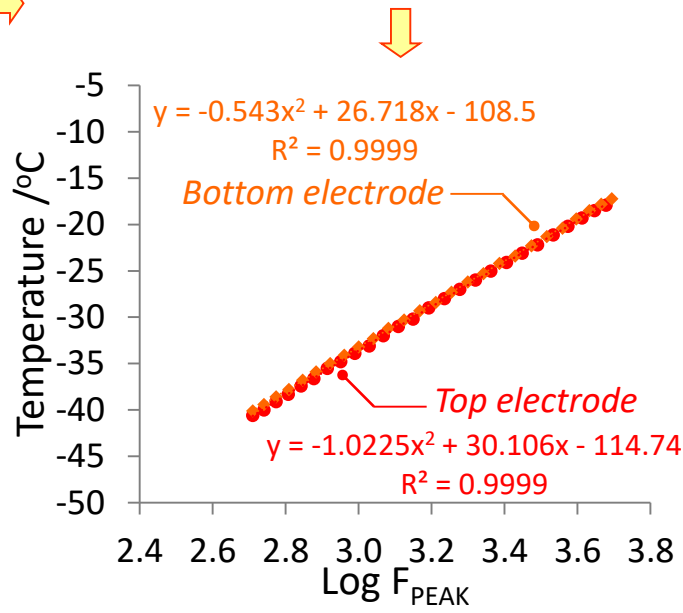
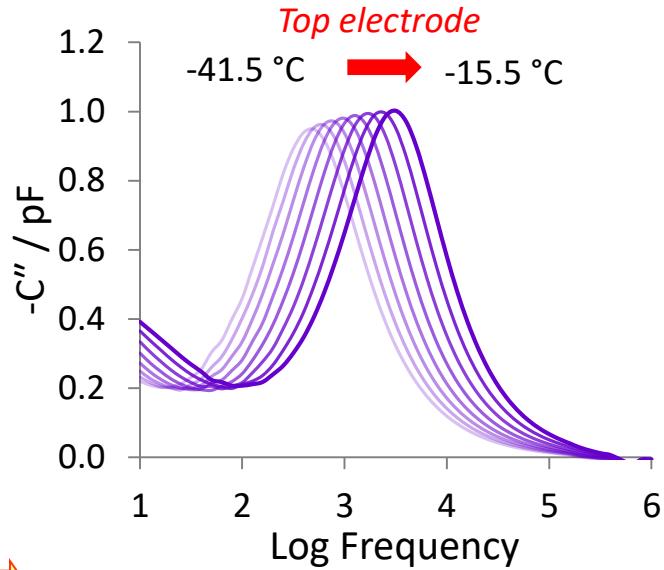
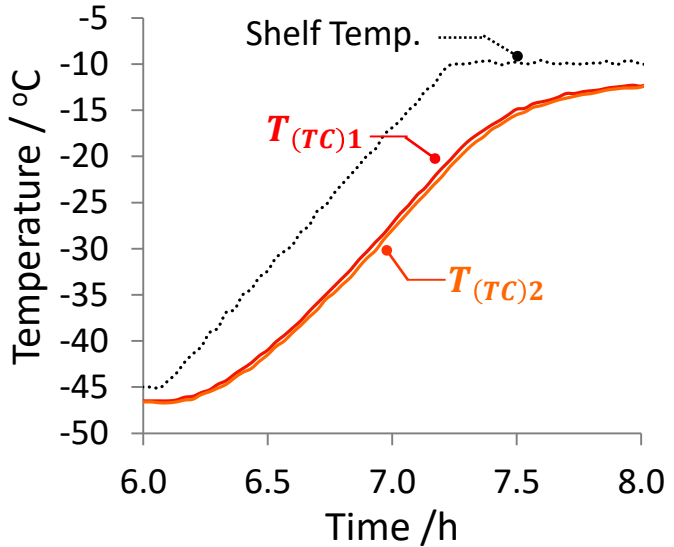
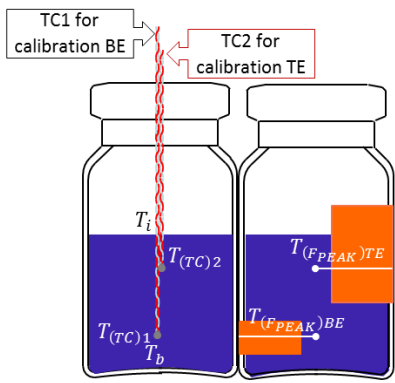
Identifying peak frequency (F_{PEAK}) using LyoView™ software

Calibration plot (temperature vs $\log F_{PEAK}$)

Predicting product temperature using calibration plot

Objective

I Temperature calibration of $\log F_{PEAK}$ of top electrode ($T_{(F_{PEAK})TE}$) and bottom electrode ($T_{(F_{PEAK})BE}$)



Polynomial coefficient from $\log F_{PEAK}$ – temperature calibration

	a	b	c
TE	-1.02	30.1	-114
BE	-5.43×10^{-1}	26.7	-109

Objective

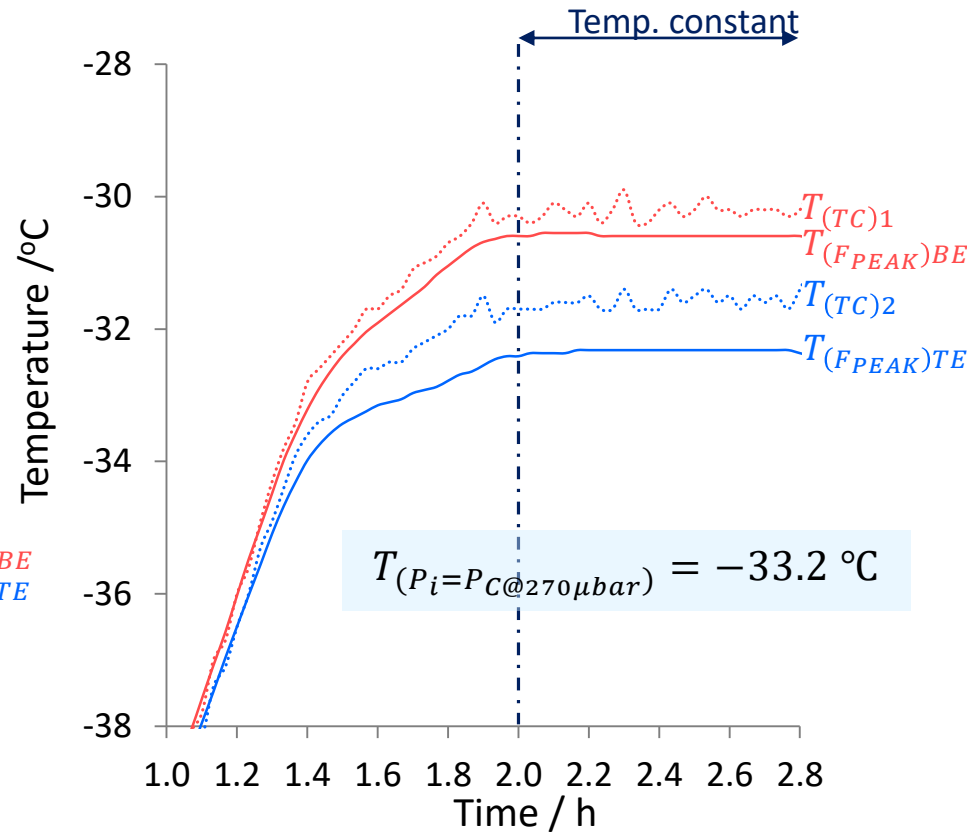
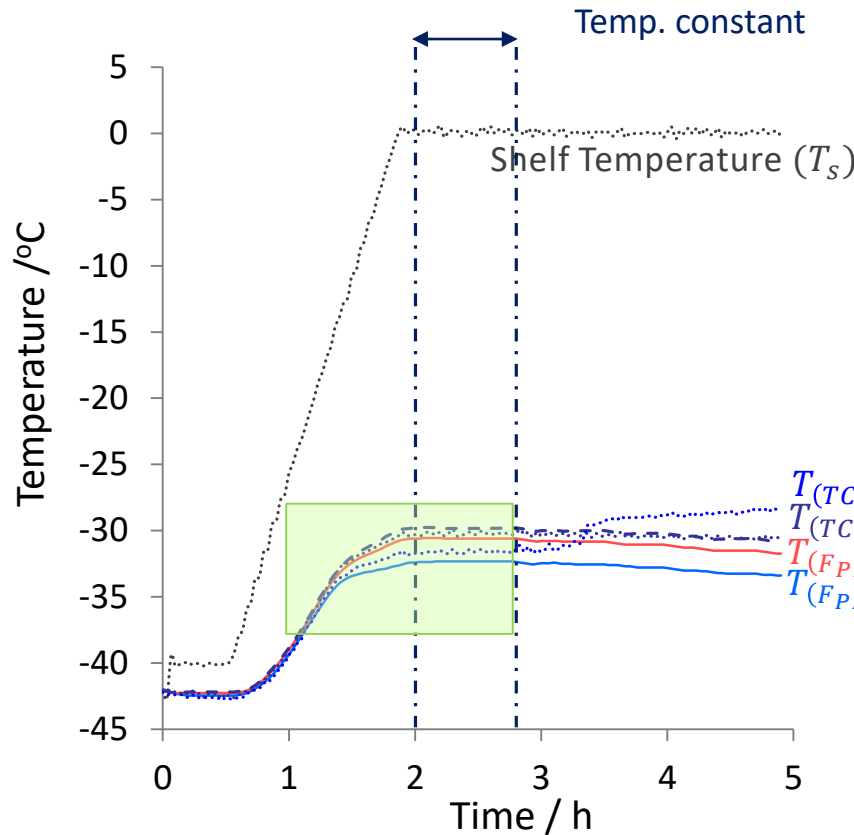
II

Prediction ice temperatures for both electrodes during primary drying

Objective

II

Prediction ice temperatures for both electrodes during primary drying



The product temperature predicted by TVIS can demonstrate the temperature gradient across ice cylinder height

Objective

III Temperature calibration of C''_{PEAK}

Annealing the sample

In-line TVIS measurement

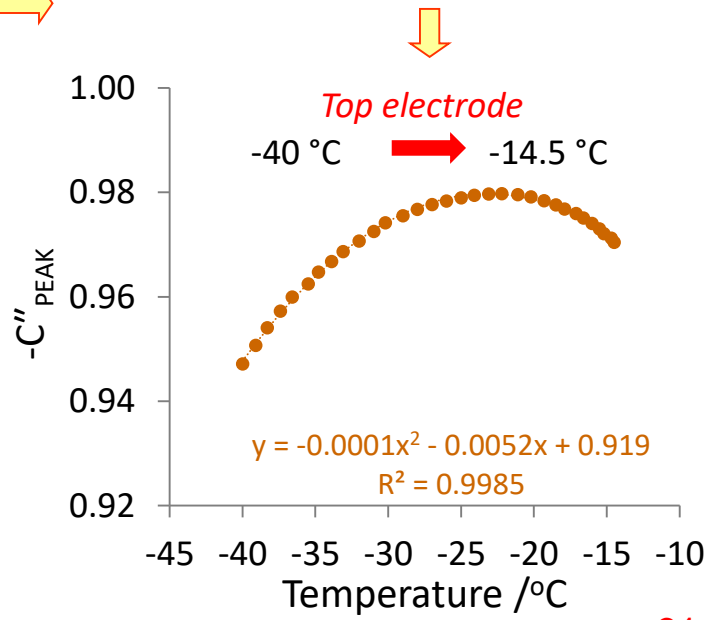
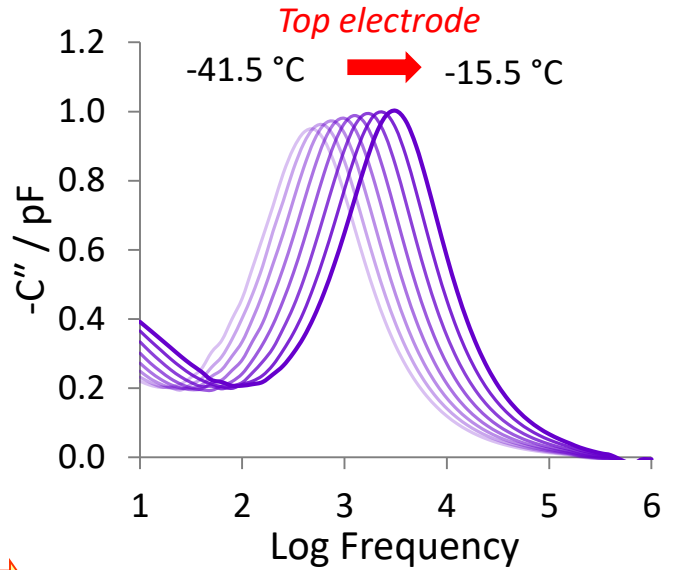
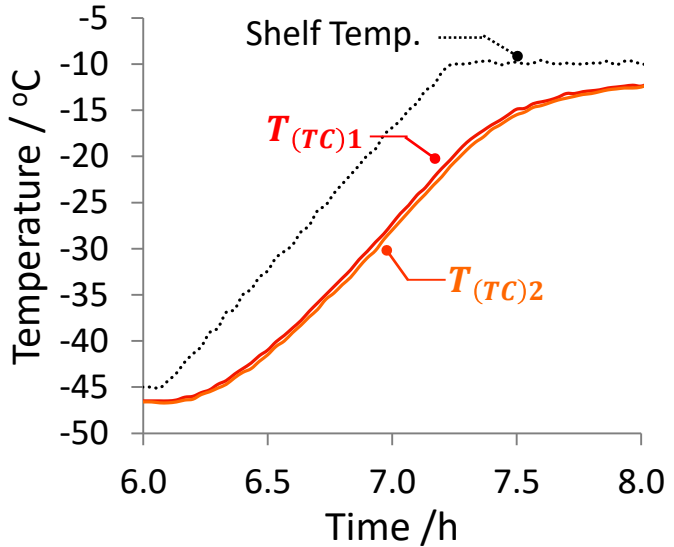
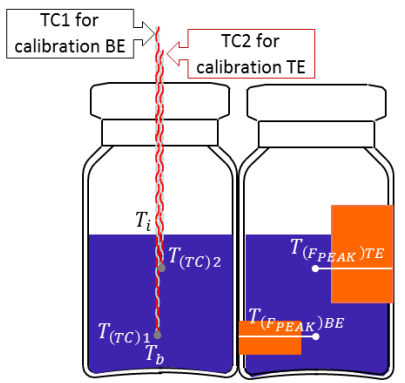
Identifying peak amplitude (C''_{PEAK}) using LyoView™ software

Calibration plot (C''_{PEAK} vs temperature)

Temperature compensation of C''_{PEAK} using calibration plot

III

Temperature calibration of C''_{PEAK}



Polynomial coefficient from C''_{PEAK} – temperature calibration

a	b	c
-1.00×10^{-4}	-5.20×10^{-3}	9.19×10^{-1}

Objective**IV**Compensation of C''_{PEAK} during primary drying

Objective

IV

Compensation of C''_{PEAK} during primary drying

- During primary drying, C''_{PEAK} is attributed to both the loss of ice and product temperature; therefore, it requires a standardization factor (ϕ) for temperature compensation:

$$\phi(T) = \frac{C''_{PEAK}(T)}{C''_{PEAK}(T_{ref})}$$

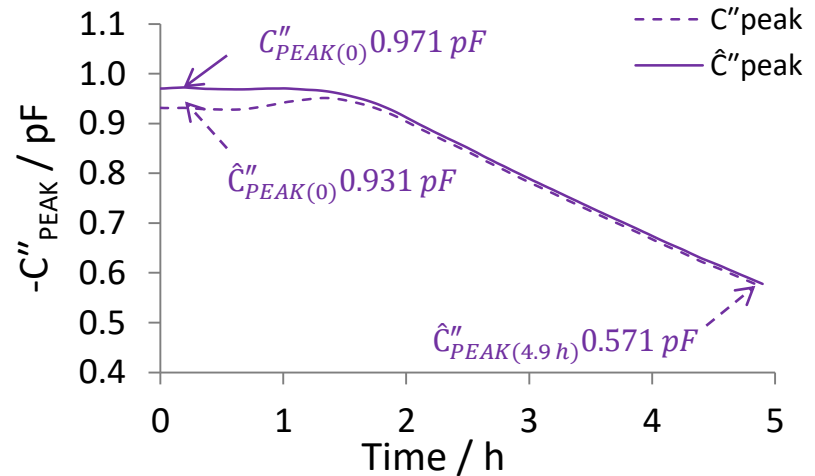
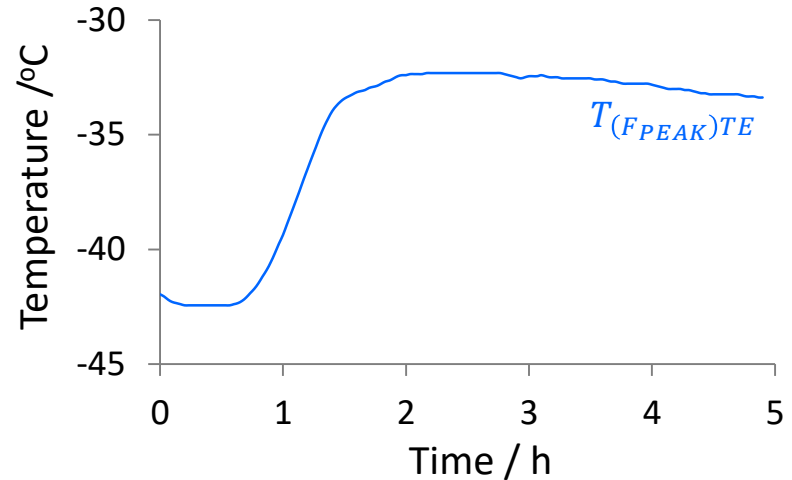
$C''_{PEAK}(T)$ and $C''_{PEAK}(T_{ref})$ are the peak amplitudes at temperatures (T) and reference temperature (T_{ref}) during the re-heating ramp. In this presentation, a temperature of $-20\text{ }^{\circ}\text{C}$ is used as the reference temperature value

- The expression for $\phi(T)$ can be re-written in terms of the polynomial coefficients (slide 22):

$$\phi(T) = \frac{aT^2 + bT + c}{aT_{ref}^2 + bT_{ref} + c}$$

- Values of C''_{PEAK} during primary drying are then standardized to the reference temperature by dividing by $\phi(T)$ to give a standardized peak amplitude of \hat{C}''_{PEAK}

$$\hat{C}''_{PEAK} = \frac{C''_{PEAK}(T)}{\phi(T)}$$



The standardized C''_{PEAK} is defined as \hat{C}''_{PEAK}

Objective

V

Calibration of C''_{PEAK} for ice layer height

Filling water into TVIS vial

Freezing the sample

In-line TVIS measurement

Thawing the sample

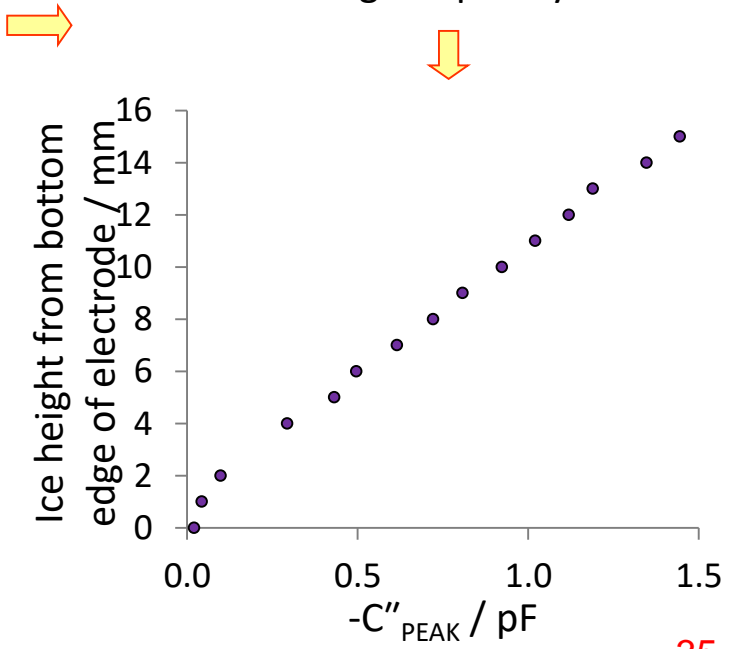
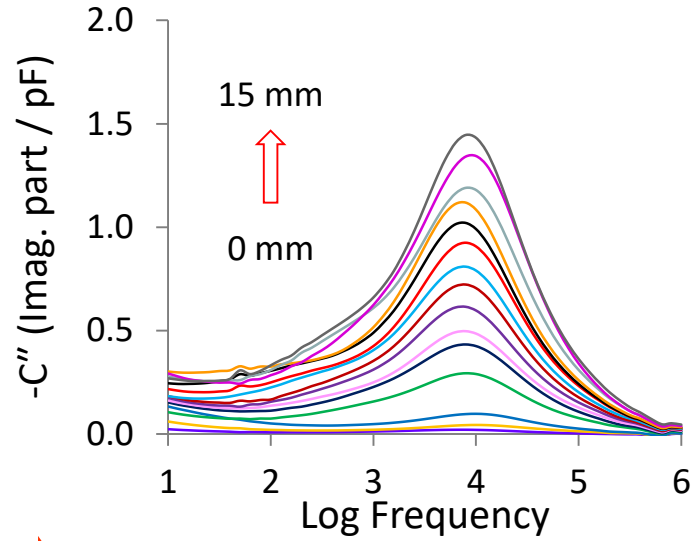
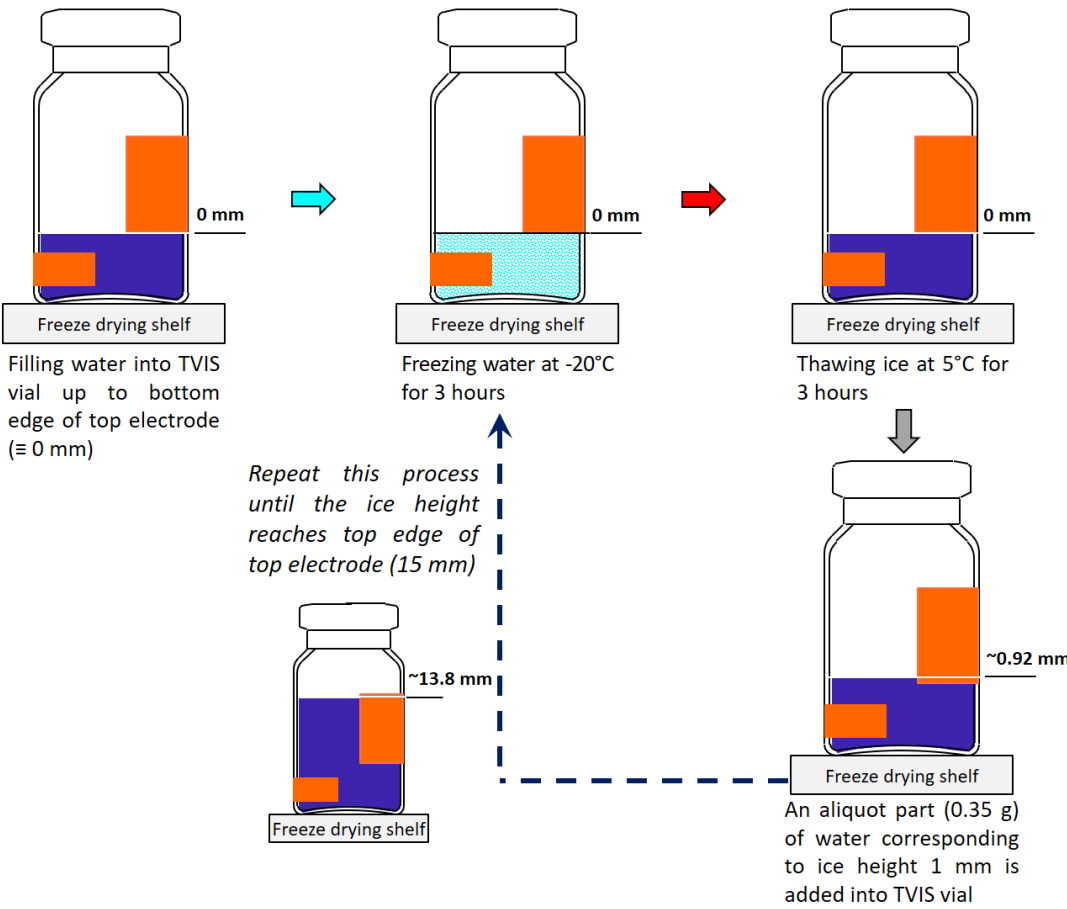
Identifying C''_{PEAK} using simple peak finding

Calibration plot (C''_{PEAK} vs temperature)



Objective

V Calibration of C''_{PEAK} for ice layer height



Objective

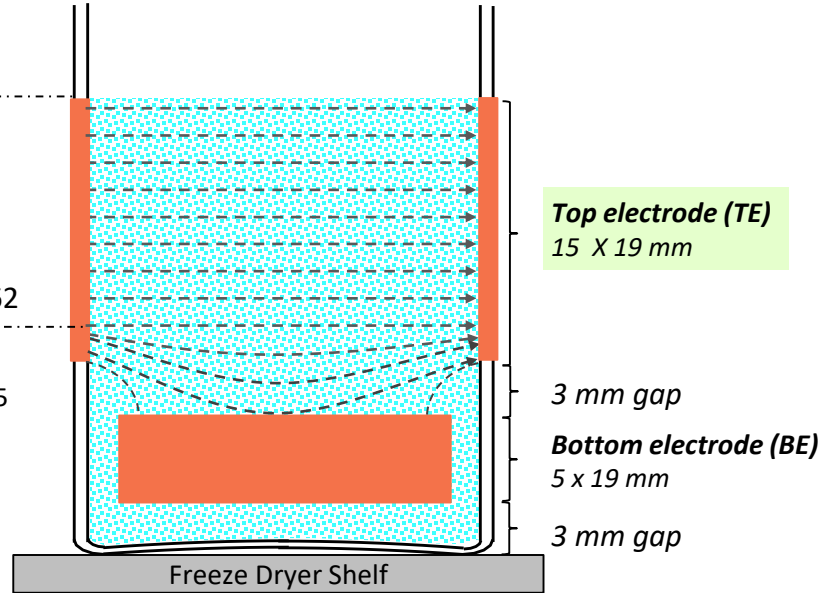
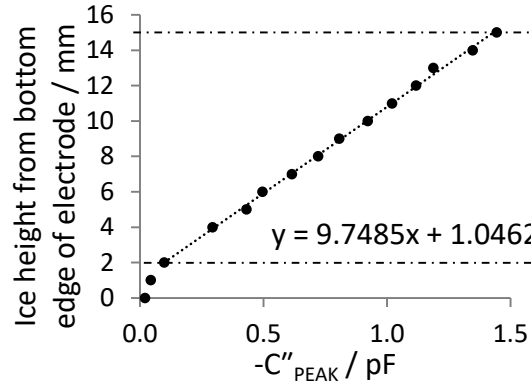
VI

Estimation of ice layer height during primary drying

Objective

VI Estimation of ice layer height during primary drying

At -20 °C



$$Ice\ height(h) = 9.7485 \times C''_{PEAK} + 1.0462$$

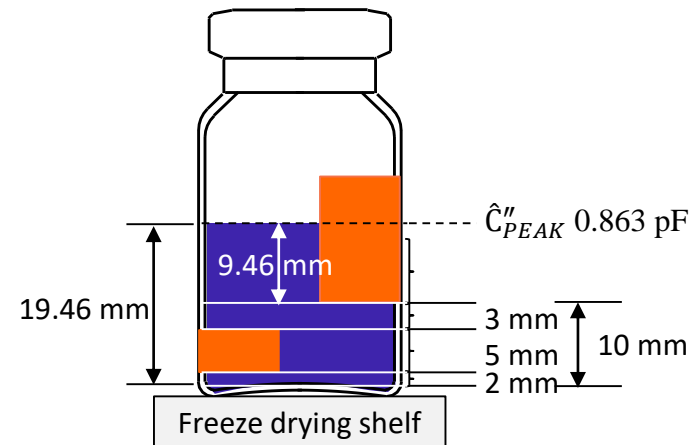
Gradient of the line ($m_{h/c}$)

At 2.4 h into primary drying

$$\hat{C}''_{PEAK} = 0.863\ pF$$

$$Ice\ height = 9.7485 \times 0.863 + 1.0462 = 9.459\ mm\ (from\ the\ bottom\ edge\ of\ TE)$$

$$Ice\ front\ height = 9.459 + (2 + 5 + 3) = 19.46\ mm$$

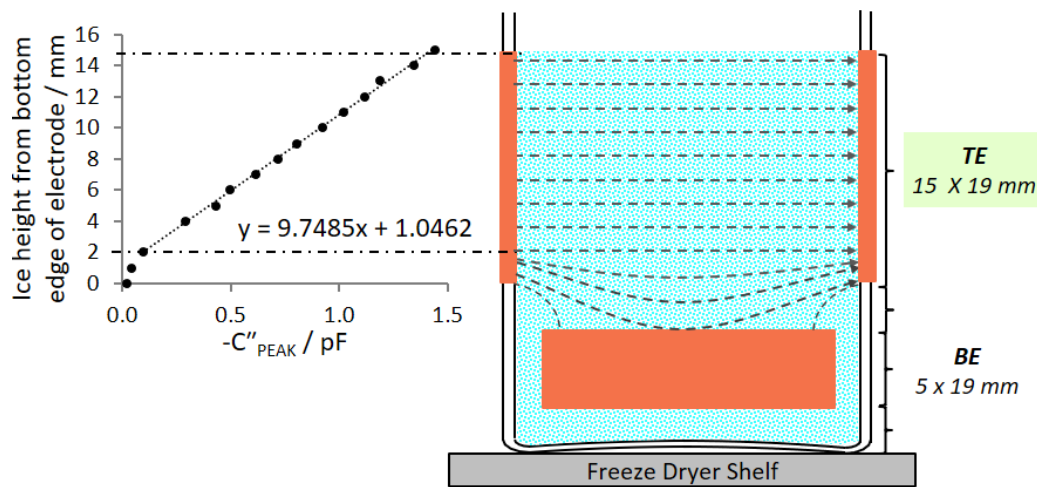


Objective

VI

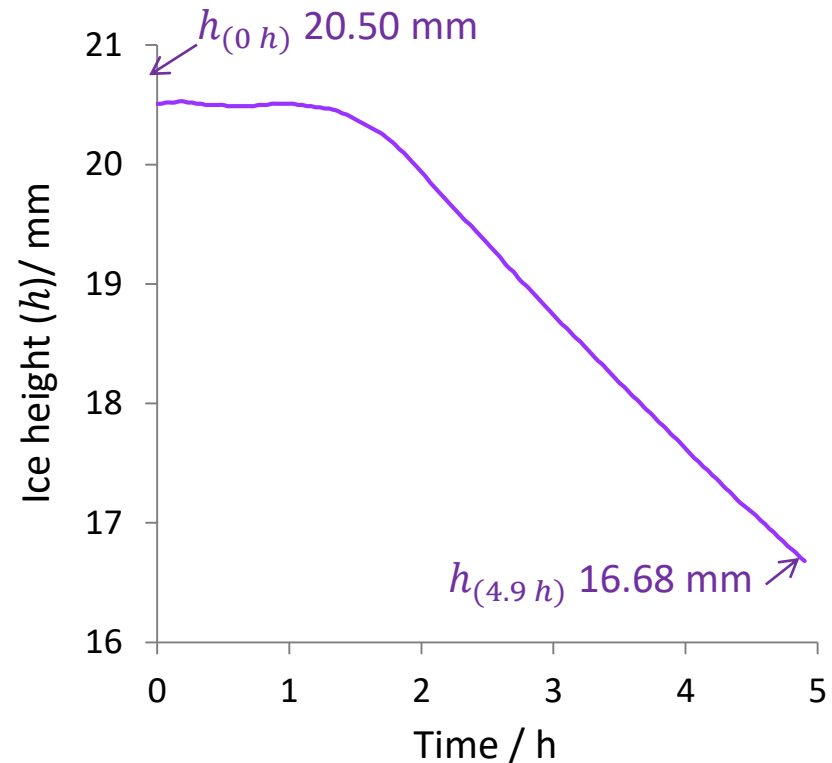
Estimation of ice layer height during primary drying

- The dependency of C''_{PEAK} on the ice cylinder height in linear region
- Surrogate drying rate can be estimated in terms of decreasing ice height



$y = 9.7485x + 1.0462$

C''_{PEAK}
 Linear gradient ($m_{h/c}$)
 Ice height (h)



Objective

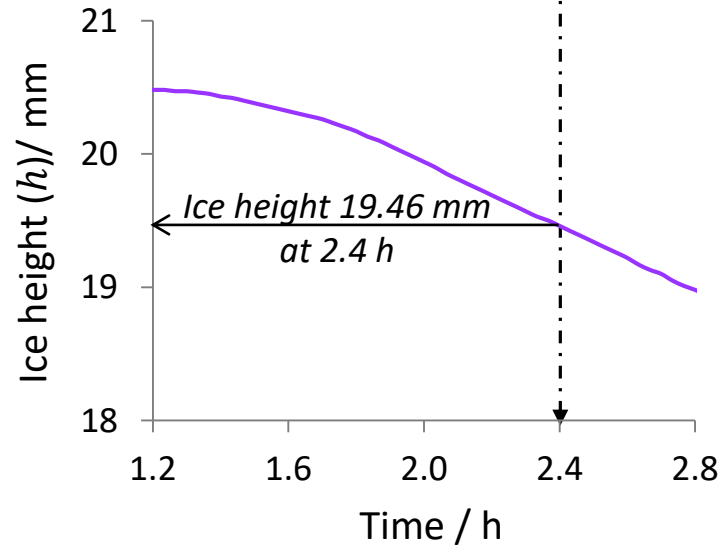
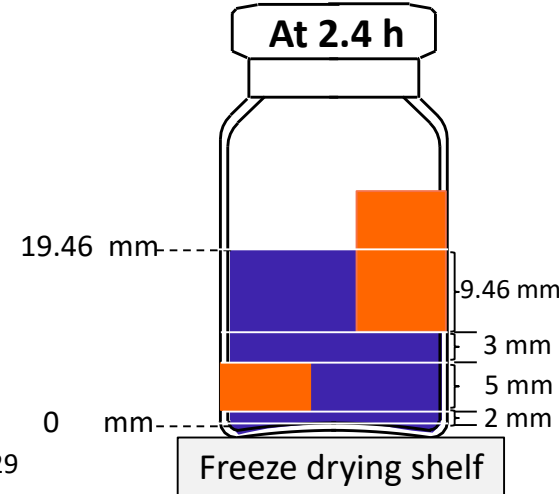
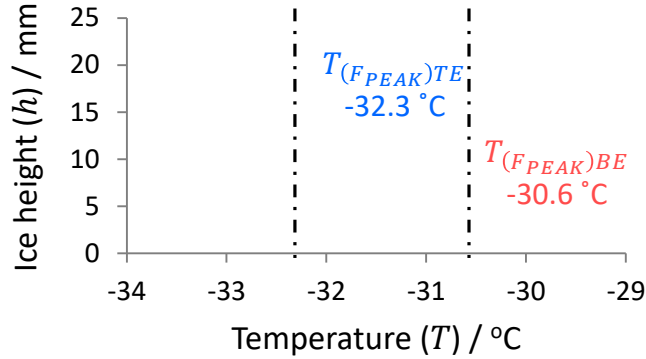
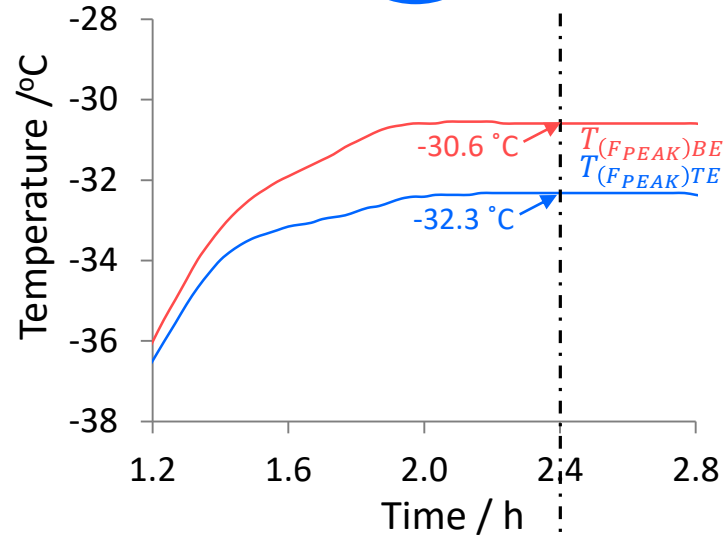
VII

Prediction ice temperatures at (i) sublimation interface (T_i) and (ii) vial's base (T_b) including qualification TVIS technique ($T_i = T_{(P_i=P_c)}$)

Objective

VII

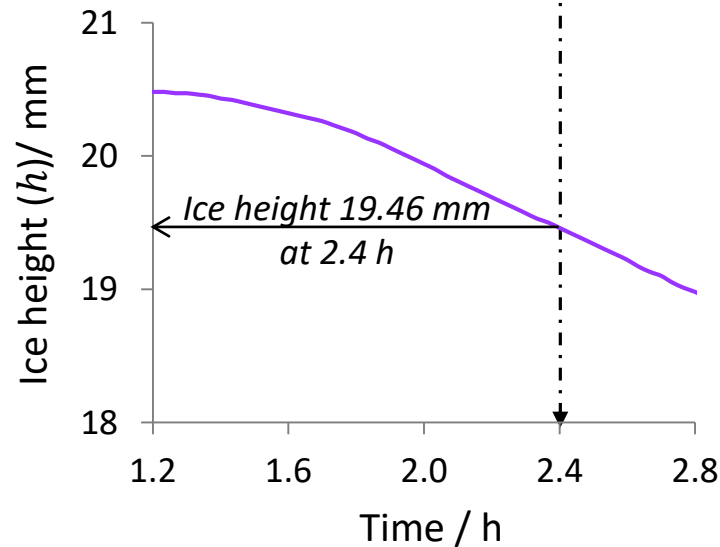
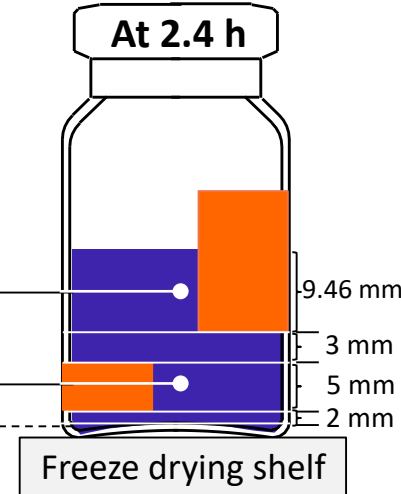
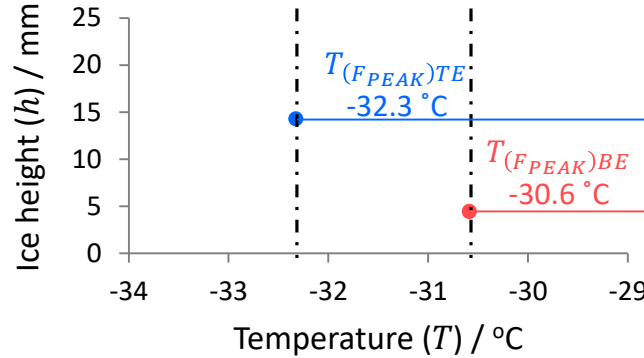
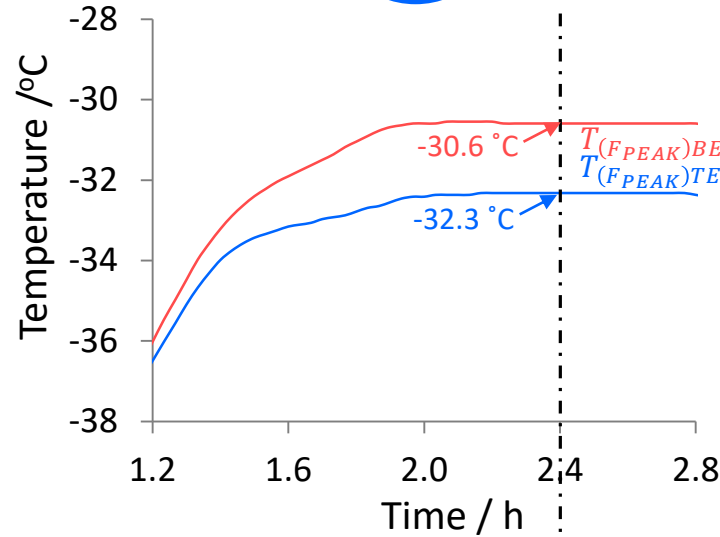
Prediction ice temperatures at (i) sublimation interface (T_i) and (ii) vial's base (T_b) including qualification TVIS technique ($T_i = T_{(P_i=P_c)}$)



Objective

VII

Prediction ice temperatures at (i) sublimation interface (T_i) and (ii) vial's base (T_b) including qualification TVIS technique ($T_i = T_{(P_i=P_c)}$)



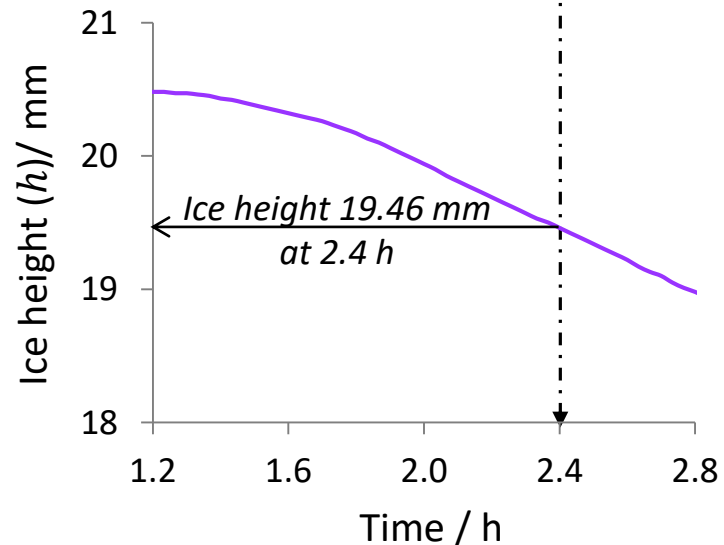
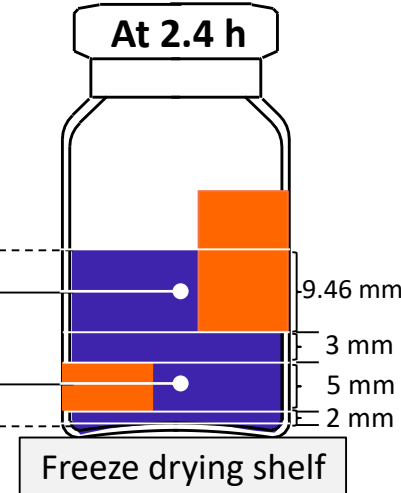
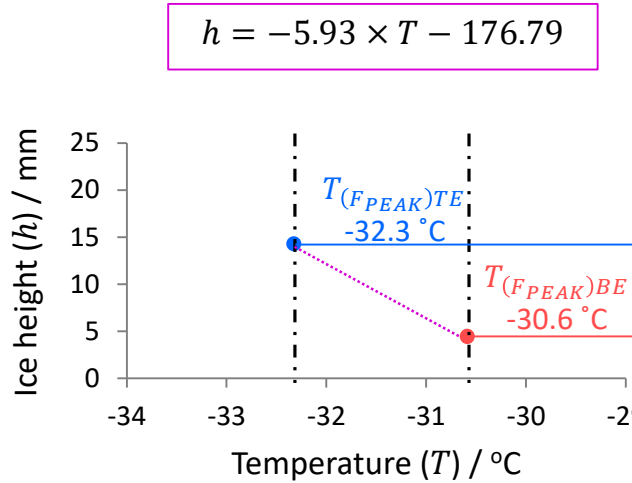
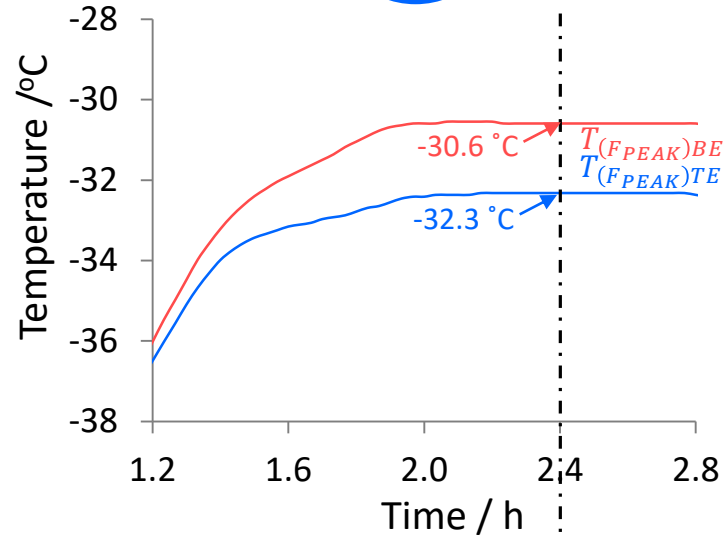
$$\text{Ice height for } T_{(FPEAK)TE} = 2 + 5 + 3 + \left(\frac{9.46}{2}\right) = 14.73 \text{ mm}$$

$$\text{Ice height for } T_{(FPEAK)BE} = 2 + \left(\frac{5}{2}\right) = 4.50 \text{ mm}$$

Objective

VII

Prediction ice temperatures at (i) sublimation interface (T_i) and (ii) vial's base (T_b) including qualification TVIS technique ($T_i = T_{(P_i=P_c)}$)



$$\text{Ice height for } T_{(FPEAK)TE} = 2 + 5 + 3 + \left(\frac{9.46}{2}\right) = 14.73 \text{ mm}$$

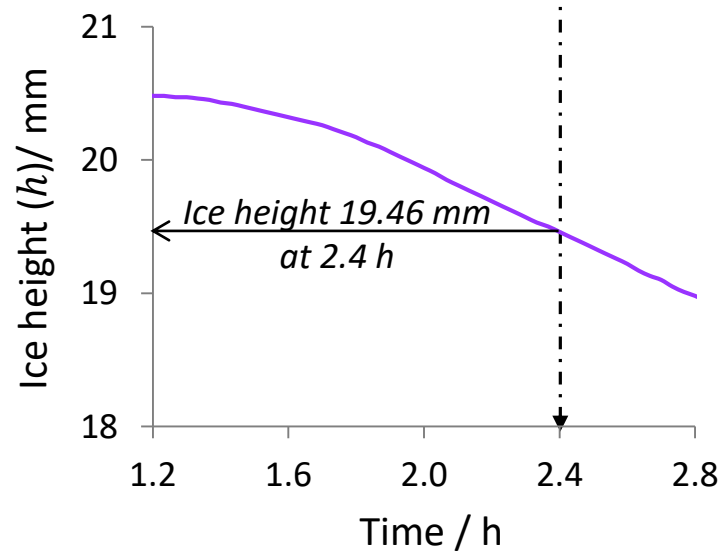
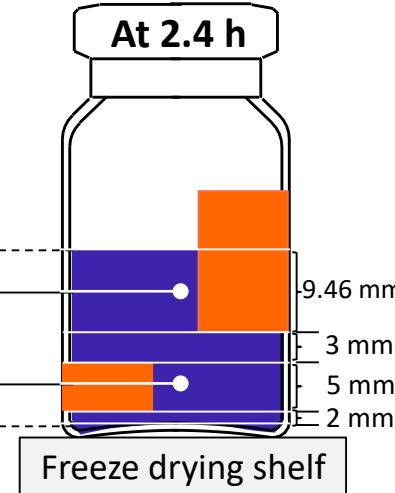
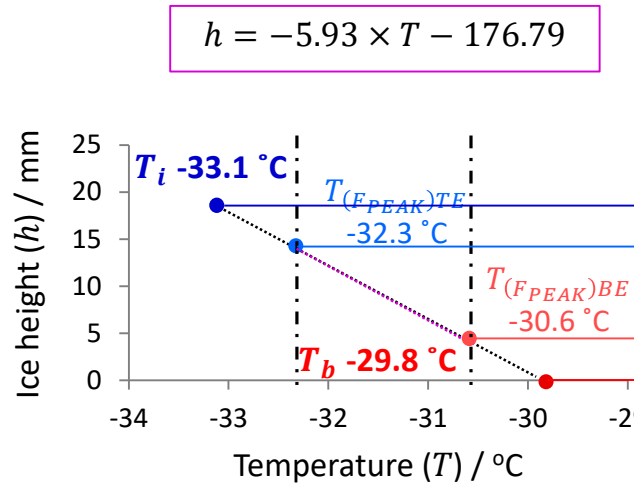
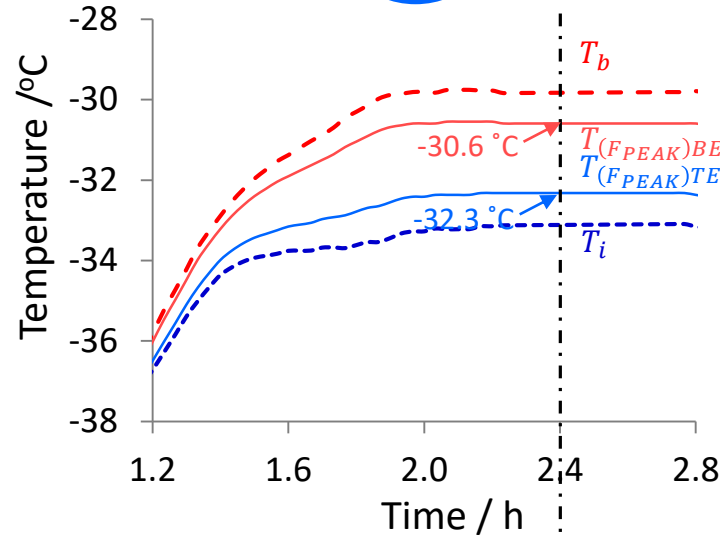
$$\text{Ice height for } T_{(FPEAK)BE} = 2 + \left(\frac{5}{2}\right) = 4.50 \text{ mm}$$

$$h = -5.93 \times T - 176.79 \quad \Rightarrow \quad T = \frac{h + 176.79}{-5.93}$$

Objective

VII

Prediction ice temperatures at (i) sublimation interface (T_i) and (ii) vial's base (T_b) including qualification TVIS technique ($T_i = T_{(P_i=P_c)}$)



Ice height for $T_{(FPEAK)TE}$ = $2 + 5 + 3 + \left(\frac{9.46}{2}\right) = 14.73$ mm

Ice height for $T_{(FPEAK)BE}$ = $2 + \left(\frac{5}{2}\right) = 4.50$ mm

$h = -5.93 \times T - 176.79$ \Rightarrow $T = \frac{h + 176.79}{-5.93}$

Ice Temperature

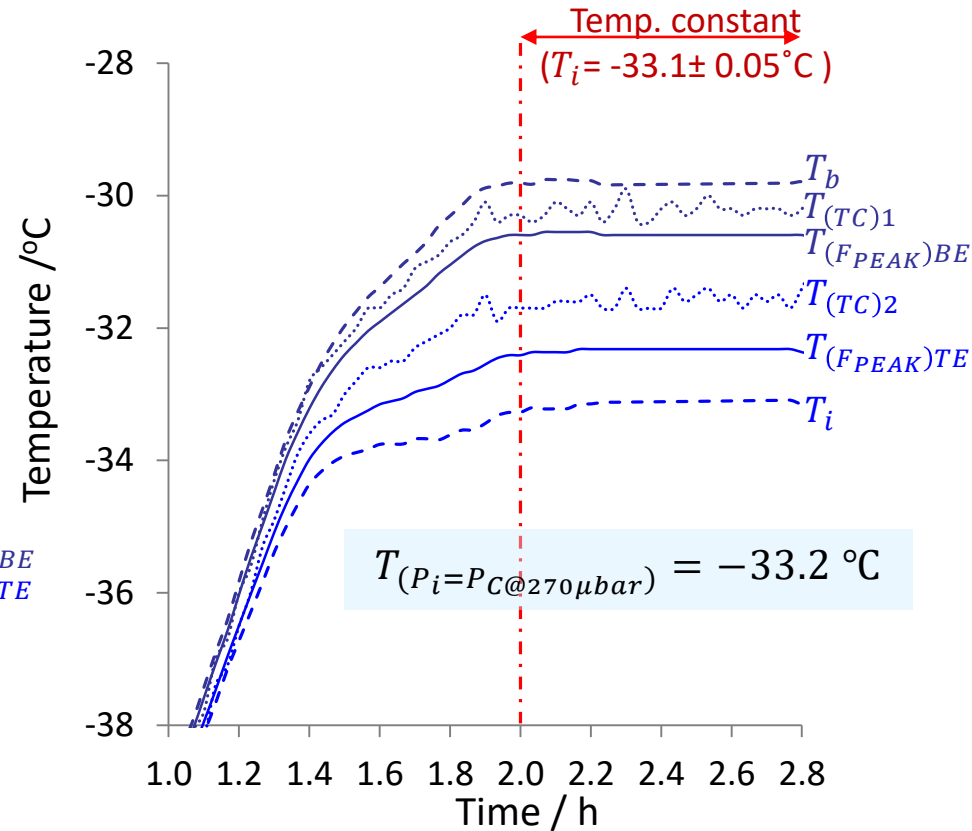
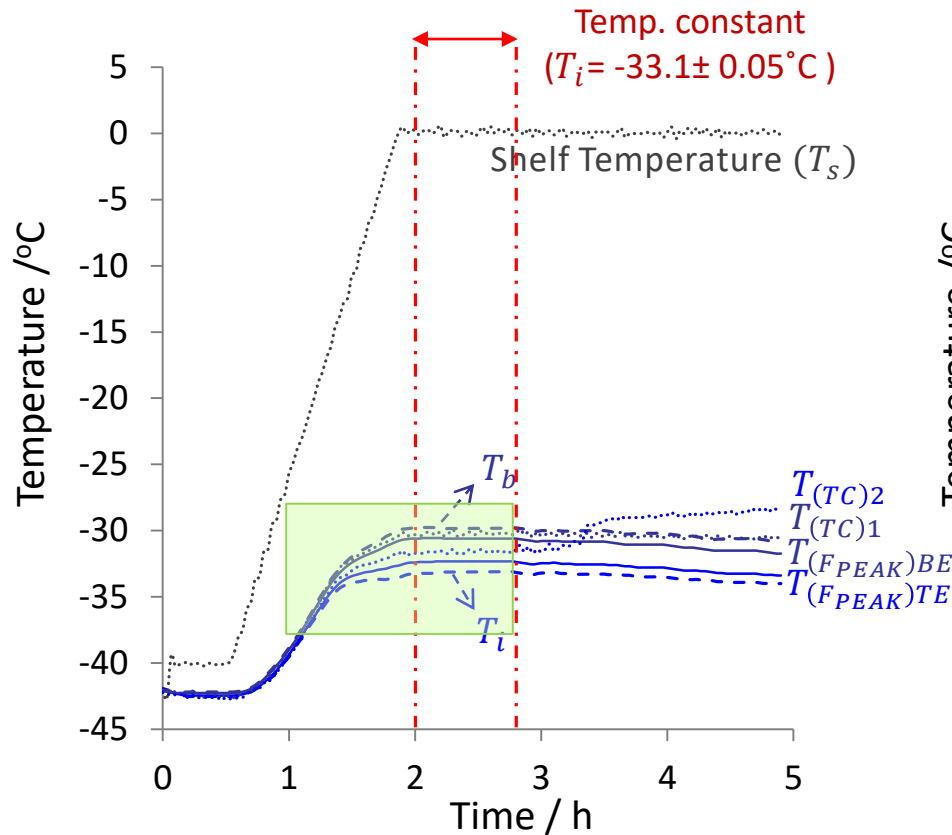
At interface ($T_i, 19.46$ mm) = $\frac{h+176.79}{-5.93} = \frac{19.46+176.79}{-5.93} = -33.1$ °C

At vial's base ($T_b, 0$ mm) = $\frac{h+176.79}{-5.93} = \frac{0+176.79}{-5.93} = -29.8$ °C

Objective

VII

Prediction ice temperatures at (i) sublimation interface (T_i) and (ii) vial's base (T_b) including qualification TVIS technique ($T_i = T_{(P_i=P_C)}$)



The product temperature at ice interface predicted by using a 2-points temperature extrapolation close to the temperature of ice vapour at chamber pressure of 270 μbar ($T_{(P_i=P_C@270\mu\text{bar})}$)

Objective

VIII

Comparison of TVIS drying rate ($\Delta m/\Delta t$) with gravimetric method (weight loss)

- Drying rate is based on the assumption of a planar sublimation front
- The change in ice cylinder height (h) can be equated to the change in ice volume (v)

$$v \text{ (cylinder)} = \pi r^2 h = Ah$$

Where r is internal radius of vial and A is internal cross section area of vial ($= \pi r^2$)

- Ice volume can be converted to ice mass (m) by multiplying with ice density (ρ_i)

$$m = \rho_i \cdot \pi r^2 h = \rho_i \cdot Ah$$

- Hence; drying rate ($\frac{\Delta m}{\Delta t}$) can be expressed by

$$\text{Drying rate } \left(\frac{\Delta m}{\Delta t} \right) = \rho_i \cdot A \cdot \frac{h_{(t1)} - h_{(t2)}}{t_2 - t_1}$$

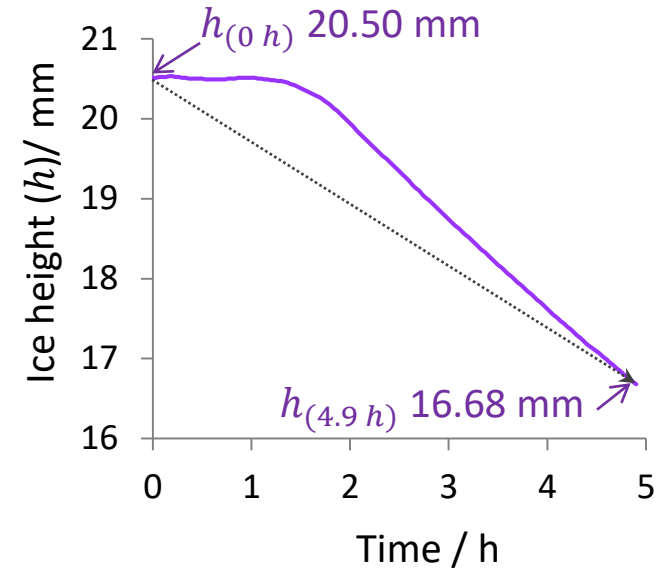
Objective VIII

Comparison of TVIS drying rate ($\Delta m/\Delta t$) with gravimetric method (weight loss)

- An average surrogate drying rate calculation

$$\text{Drying rate } \left(\frac{\Delta m}{\Delta t}\right) = \rho_i \cdot A \cdot \frac{h_{(t_1)} - h_{(t_2)}}{t_2 - t_1}$$

Ice density (ρ_i) at -32°C = $0.920 \text{ g}\cdot\text{cm}^{-3}$
 Internal vial diameter (VC010-20C) = 2.21 cm
 Cross-section area (A) = 3.80 cm^2
 Ice height at 0 h ($h_{(0 \text{ h})}$) = 20.50 mm
 Ice height at 4.9 h ($h_{(4.9 \text{ h})}$) = 16.68 mm



$$\begin{aligned} \text{Drying rate} &= 0.920 \text{ g}\cdot\text{cm}^{-3} \times 3.80 \text{ cm}^2 \times \frac{(20.50 - 16.68) \times 10^{-1} \text{ cm}}{(4.9 - 0) \text{ h}} \\ &= \mathbf{0.27 \text{ g}\cdot\text{h}^{-1}} \end{aligned}$$

	Drying rate
TVIS	0.27 g/h
Gravimetric	0.25 g/h

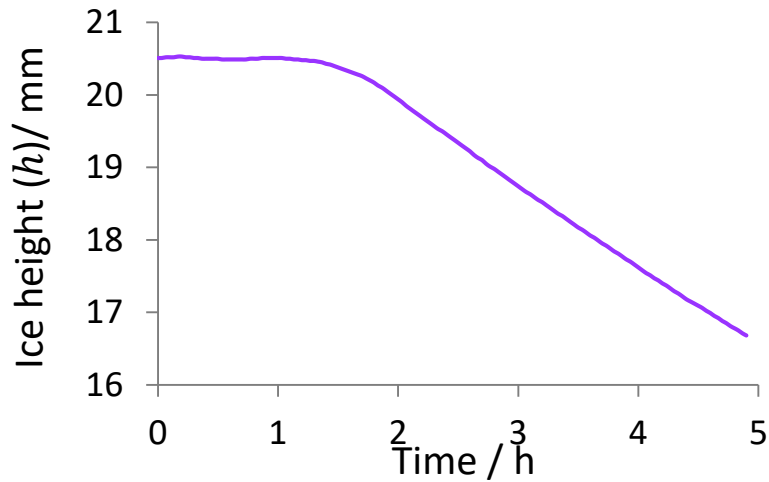
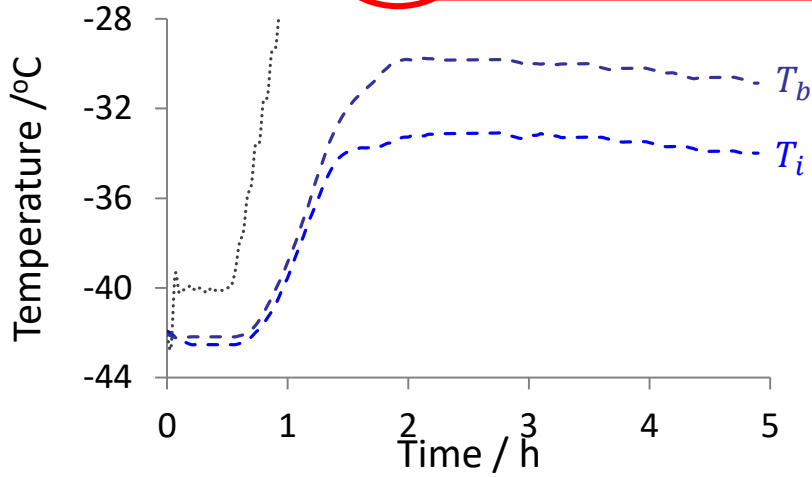
Objective

IX

Determination (i) the drying rate ($\Delta m/\Delta t$) and (ii) ice base temperature (T_b) during the steady state period

Objective

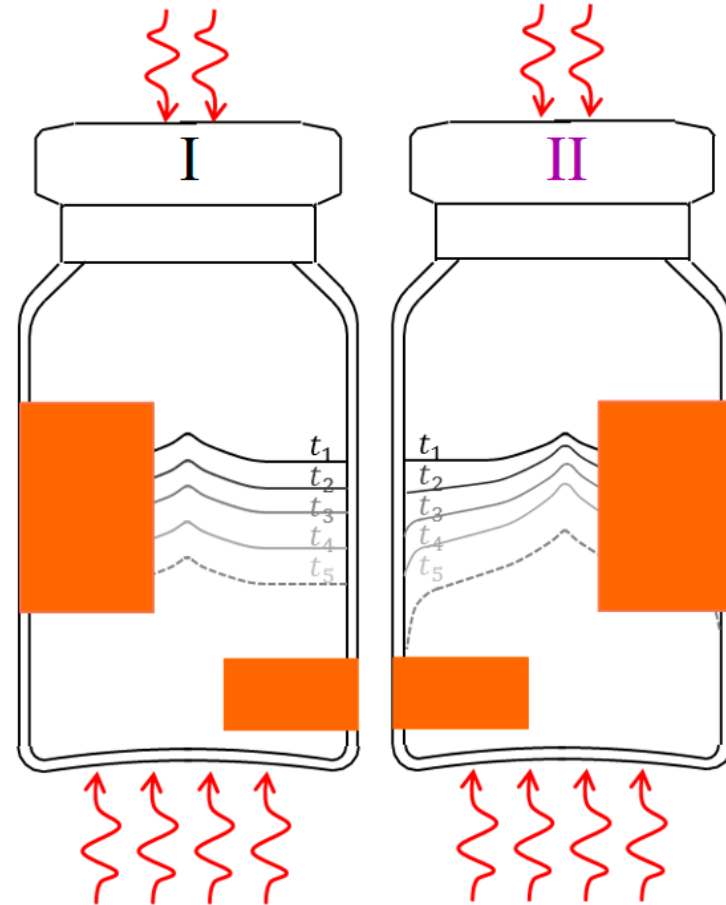
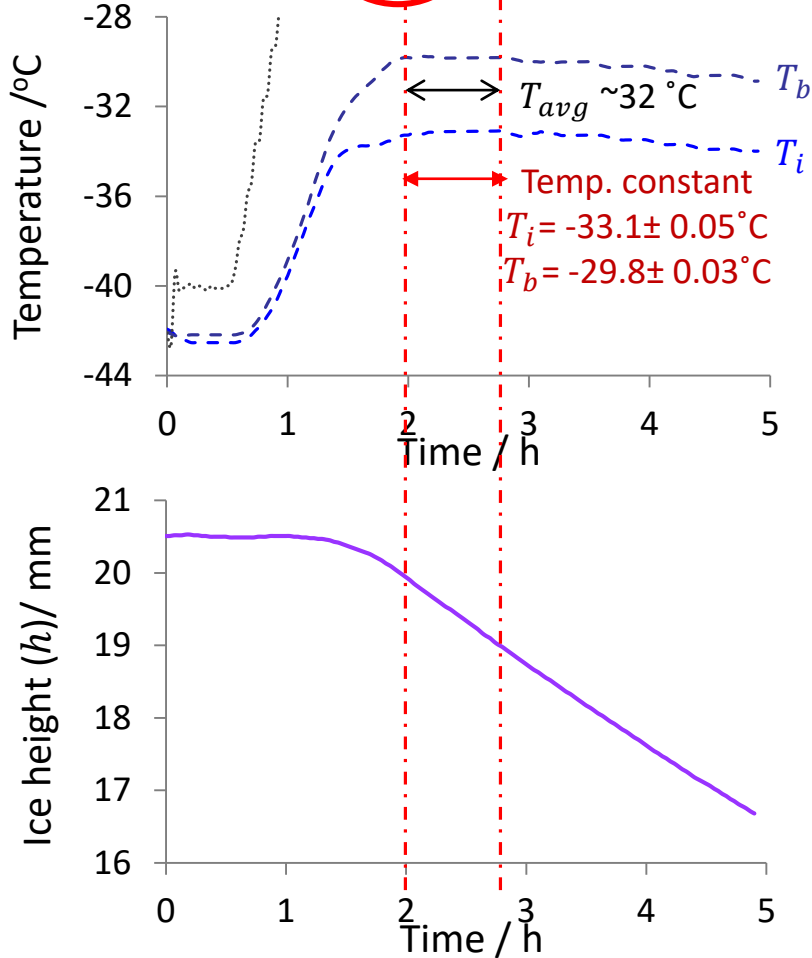
IX Determination (i) the drying rate ($\Delta m/\Delta t$) and (ii) ice base temperature (T_b) during the steady state period for heat transfer coefficient (K_v) calculation



Objective

IX

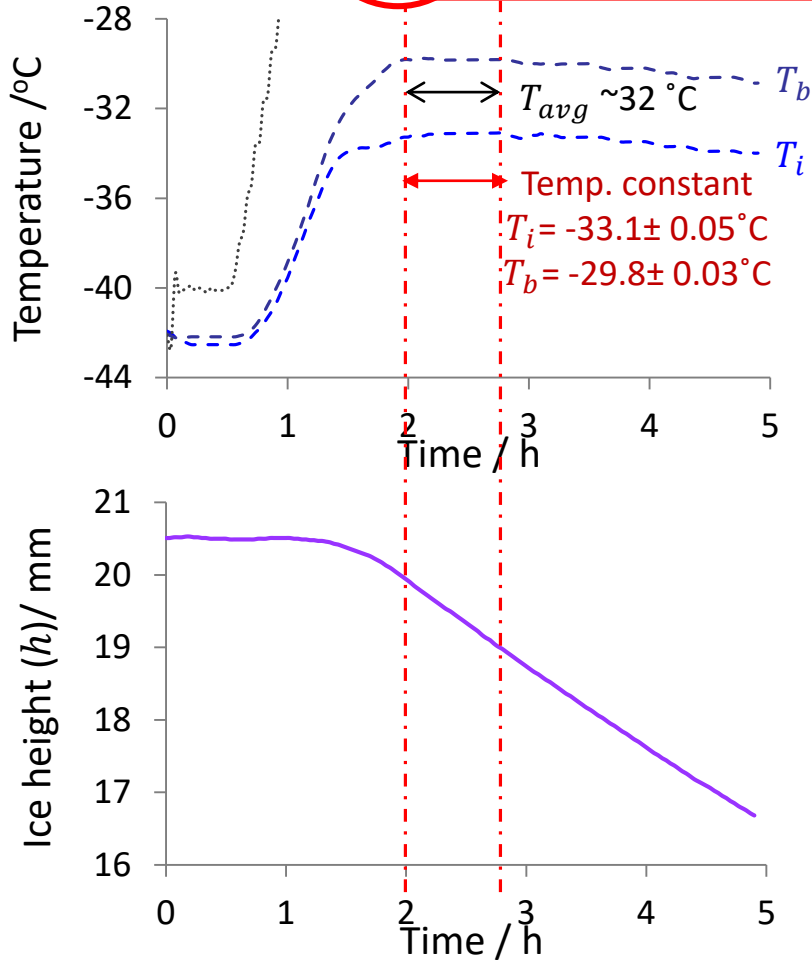
Determination (i) the drying rate ($\Delta m/\Delta t$) and (ii) ice base temperature (T_b) during the steady state period for heat transfer coefficient (K_v) calculation



Objective

IX

Determination (i) the drying rate ($\Delta m/\Delta t$) and (ii) ice base temperature (T_b) during the steady state period for heat transfer coefficient (K_v) calculation



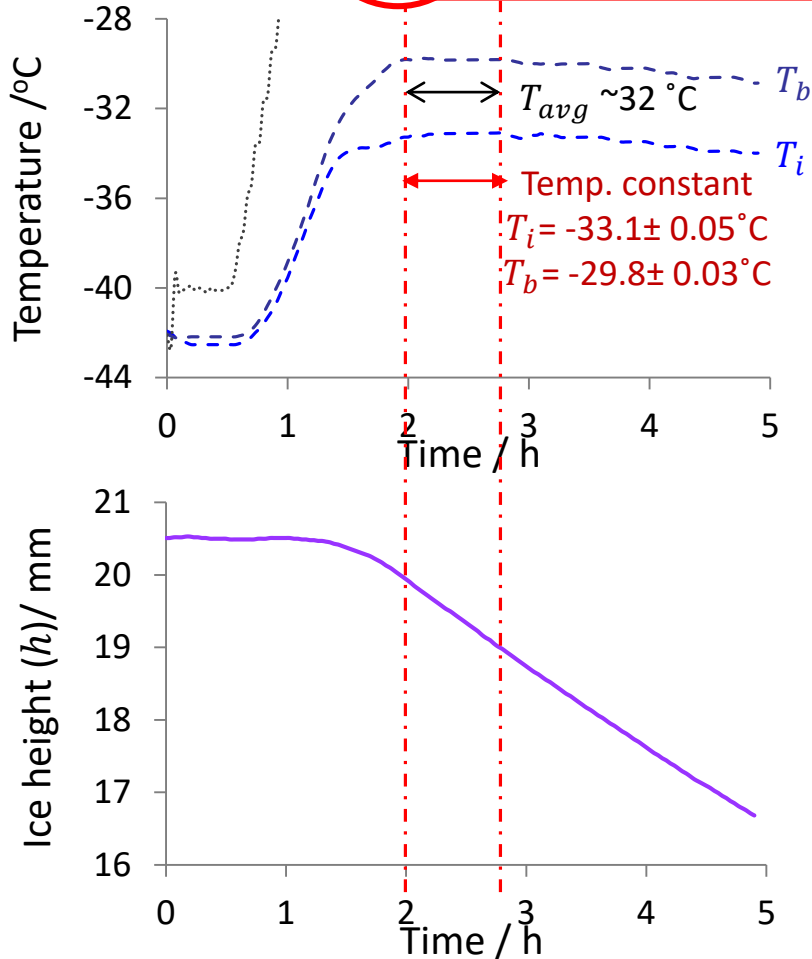
- Drying rate during the steady state

$$\text{Drying rate } \left(\frac{\Delta m}{\Delta t} \right) = \rho_i \cdot A \cdot \frac{h_{(t_1)} - h_{(t_2)}}{t_2 - t_1}$$

Objective

IX

Determination (i) the drying rate ($\Delta m/\Delta t$) and (ii) ice base temperature (T_b) during the steady state period for heat transfer coefficient (K_v) calculation



- Drying rate during the steady state

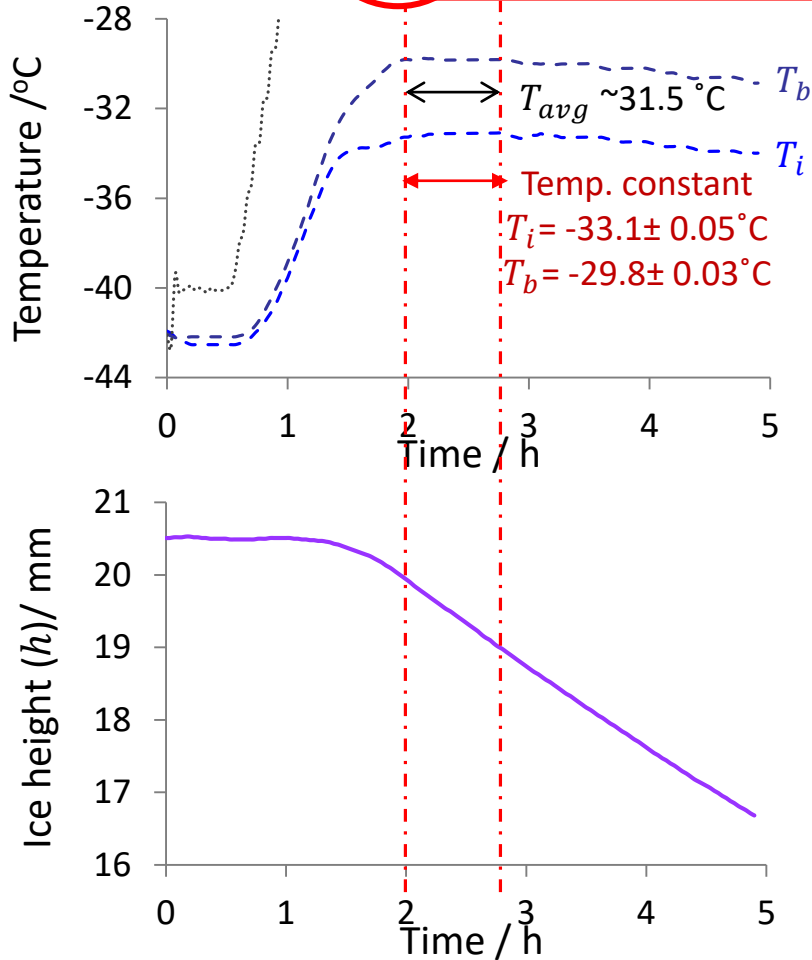
$$\text{Drying rate } \left(\frac{\Delta m}{\Delta t} \right) = \rho_i \cdot A \cdot \frac{h_{(t_1)} - h_{(t_2)}}{t_2 - t_1}$$

Ice density (ρ_i) at $-32\text{ }^{\circ}\text{C}$ = $0.920\text{ g}\cdot\text{cm}^{-3}$
 (Calculated ice temperature between T_i & T_b)

Objective

IX

Determination (i) the drying rate ($\Delta m/\Delta t$) and (ii) ice base temperature (T_b) during the steady state period for heat transfer coefficient (K_v) calculation



- Drying rate during the steady state

$$\text{Drying rate } \left(\frac{\Delta m}{\Delta t} \right) = \rho_i \cdot A \cdot \frac{h_{(t_1)} - h_{(t_2)}}{t_2 - t_1}$$

Ice density (ρ_i) at -32°C = $0.920 \text{ g}\cdot\text{cm}^{-3}$

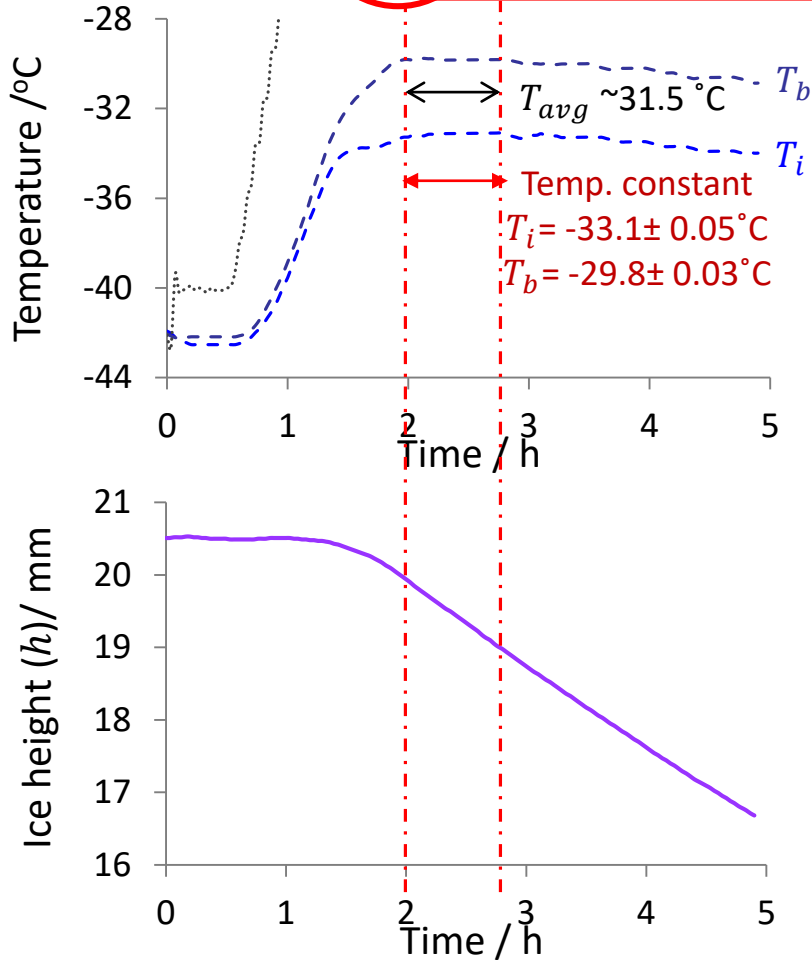
(Calculated ice temperature between T_i & T_b)

Internal vial diameter (VC010-20C) = 2.21 cm

Objective

IX

Determination (i) the drying rate ($\Delta m/\Delta t$) and (ii) ice base temperature (T_b) during the steady state period for heat transfer coefficient (K_v) calculation



- Drying rate during the steady state

$$\text{Drying rate } \left(\frac{\Delta m}{\Delta t} \right) = \rho_i \cdot A \cdot \frac{h_{(t_1)} - h_{(t_2)}}{t_2 - t_1}$$

Ice density (ρ_i) at -32°C = $0.920 \text{ g}\cdot\text{cm}^{-3}$

(Calculated ice temperature between T_i & T_b)

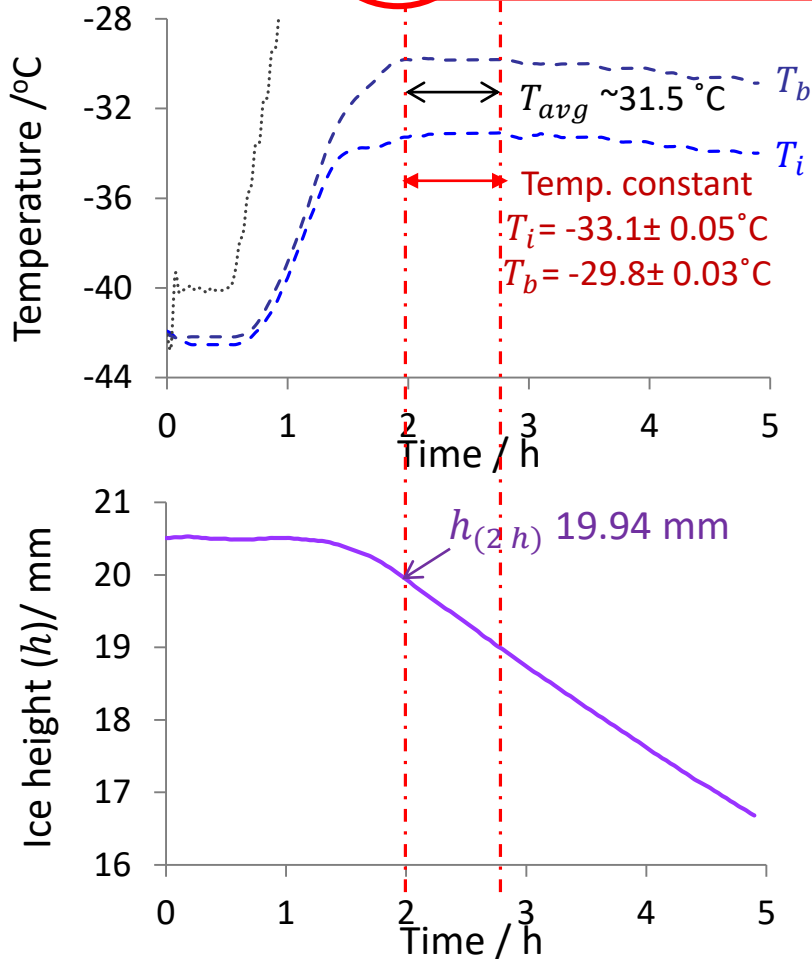
Internal vial diameter (VC010-20C) = 2.21 cm

Cross-section area (A) = 3.80 cm^2

Objective

IX

Determination (i) the drying rate ($\Delta m/\Delta t$) and (ii) ice base temperature (T_b) during the steady state period for heat transfer coefficient (K_v) calculation



- Drying rate during the steady state

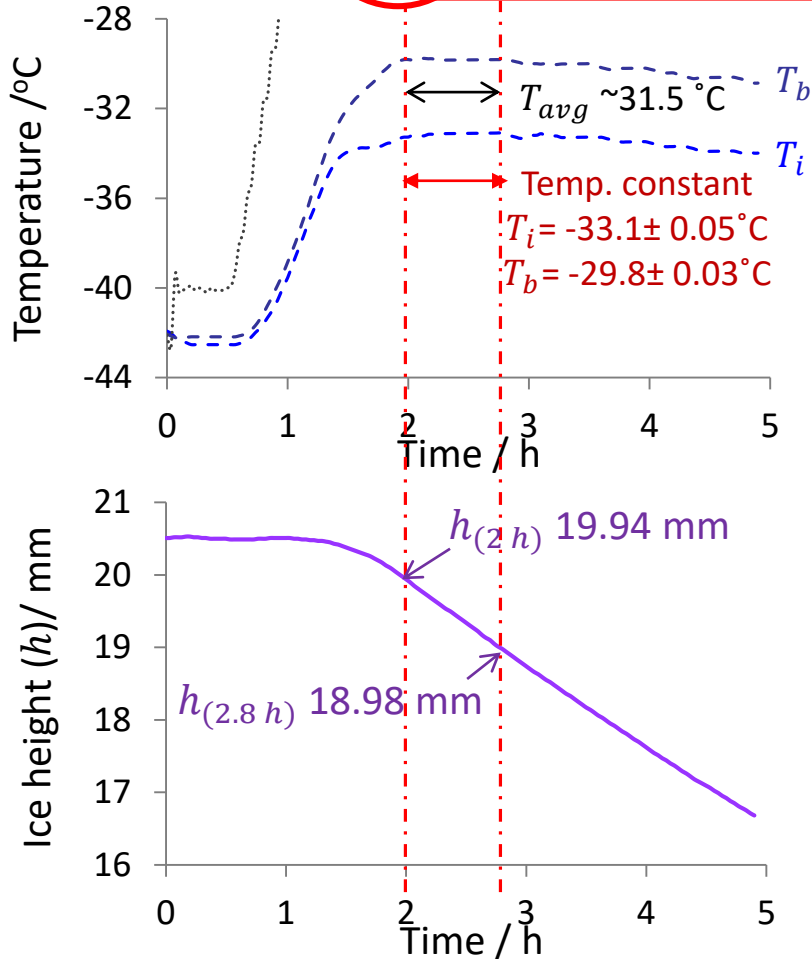
$$\text{Drying rate } \left(\frac{\Delta m}{\Delta t} \right) = \rho_i \cdot A \cdot \frac{h_{(t_1)} - h_{(t_2)}}{t_2 - t_1}$$

Ice density (ρ_i) at -32°C = $0.920 \text{ g}\cdot\text{cm}^{-3}$
(Calculated ice temperature between T_i & T_b)
 Internal vial diameter (VC010-20C) = 2.21 cm
 Cross-section area (A) = 3.80 cm^2
 Ice height at 2 h ($h_{(2h)}$) = 19.94 mm

Objective

IX

Determination (i) the drying rate ($\Delta m/\Delta t$) and (ii) ice base temperature (T_b) during the steady state period for heat transfer coefficient (K_v) calculation



- Drying rate during the steady state

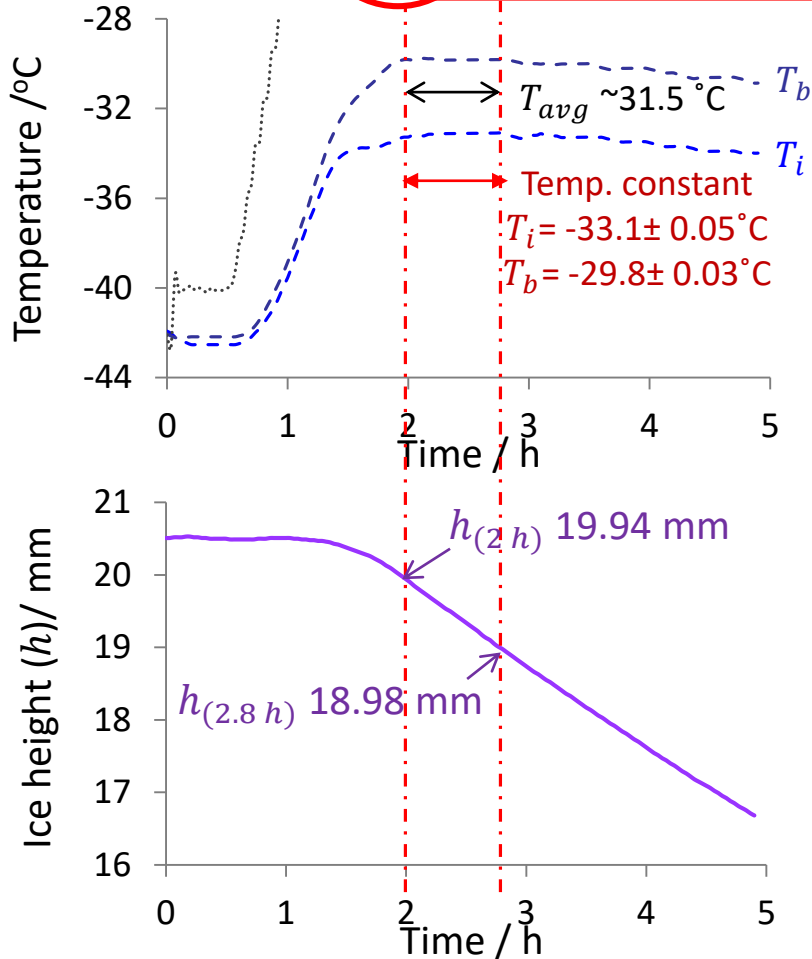
$$\text{Drying rate } \left(\frac{\Delta m}{\Delta t}\right) = \rho_i \cdot A \cdot \frac{h_{(t_1)} - h_{(t_2)}}{t_2 - t_1}$$

Ice density (ρ_i) at -32°C = $0.920\text{ g}\cdot\text{cm}^{-3}$
 (Calculated ice temperature between T_i & T_b)
 Internal vial diameter (VC010-20C) = 2.21 cm
 Cross-section area (A) = 3.80 cm^2
 Ice height at 2 h ($h_{(2h)}$) = 19.94 mm
 Ice height at 2.8 h ($h_{(2.8h)}$) = 18.98 mm

Objective

IX

Determination (i) the drying rate ($\Delta m/\Delta t$) and (ii) ice base temperature (T_b) during the steady state period for heat transfer coefficient (K_v) calculation



- Drying rate during the steady state

$$\text{Drying rate } \left(\frac{\Delta m}{\Delta t} \right) = \rho_i \cdot A \cdot \frac{h_{(t_1)} - h_{(t_2)}}{t_2 - t_1}$$

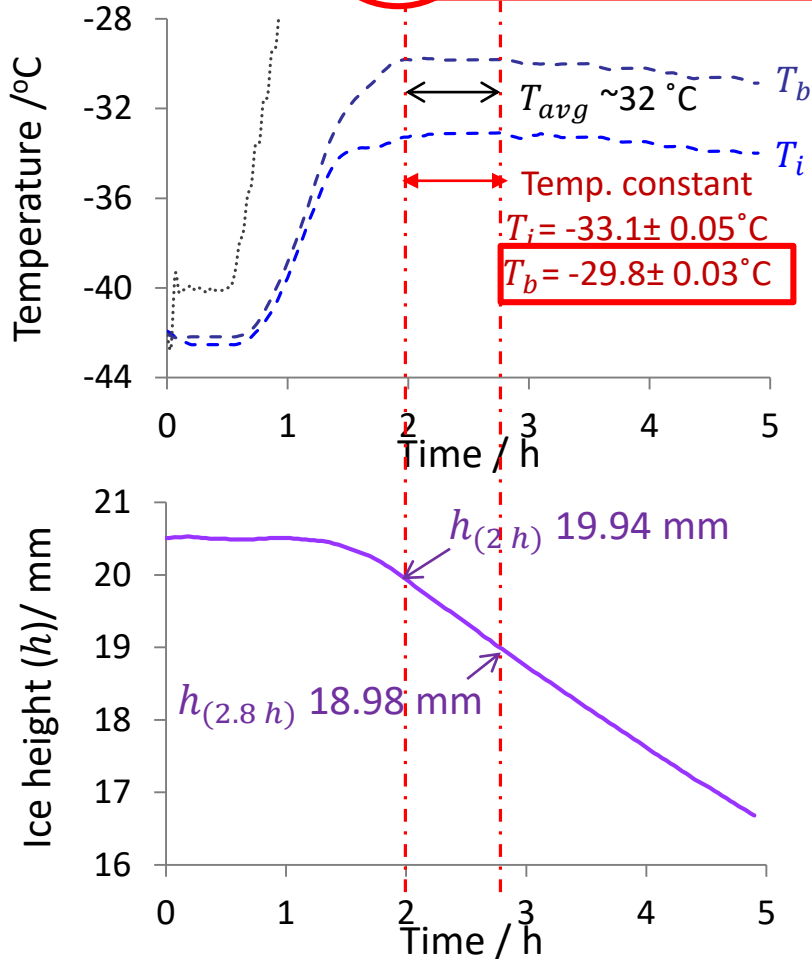
Ice density (ρ_i) at -32°C	= $0.920 \text{ g} \cdot \text{cm}^{-3}$
<i>(Calculated ice temperature between T_i & T_b)</i>	
Internal vial diameter (VC010-20C)	= 2.21 cm
Cross-section area (A)	= 3.80 cm^2
Ice height at 2 h ($h_{(2h)}$)	= 19.94 mm
Ice height at 2.8 h ($h_{(2.8h)}$)	= 18.98 mm

$$\begin{aligned} \text{Drying rate} &= 0.920 \text{ g} \cdot \text{cm}^{-3} \times 3.80 \text{ cm}^2 \times \frac{(19.94 - 18.98) \times 10^{-1} \text{ cm}}{(2.8 - 2.0) \text{ h}} \\ &= \mathbf{0.42 \text{ g} \cdot \text{h}^{-1}} \end{aligned}$$

Objective

IX

Determination (i) the drying rate ($\Delta m/\Delta t$) and (ii) ice base temperature (T_b) during the steady state period for heat transfer coefficient (K_v) calculation



- Drying rate during the steady state

$$\text{Drying rate } \left(\frac{\Delta m}{\Delta t}\right) = \rho_i \cdot A \cdot \frac{h_{(t_1)} - h_{(t_2)}}{t_2 - t_1}$$

Ice density (ρ_i) at -32°C = $0.920 \text{ g}\cdot\text{cm}^{-3}$

(Calculated ice temperature between T_i & T_b)

Internal vial diameter (VC010-20C) = 2.21 cm

Cross-section area (A) = 3.80 cm^2

Ice height at 2 h ($h_{(2h)}$) = 19.94 mm

Ice height at 2.8 h ($h_{(2.8h)}$) = 18.98 mm

TVIS parameters used for determination:

$$\frac{\Delta m}{\Delta t} = 0.42 \text{ g}\cdot\text{h}^{-1}$$

$$T_b = -29.8^\circ\text{C}$$

$$\text{Drying rate} = 0.920 \text{ g}\cdot\text{cm}^{-3} \times 3.80 \text{ cm}^2 \times \frac{(19.94 - 18.98) \times 10^{-1} \text{ cm}}{(2.8 - 2.0) \text{ h}}$$

$$= 0.42 \text{ g}\cdot\text{h}^{-1}$$

Objective

X

Heat transfer coefficient (K_v) calculation

Objective

X

Heat transfer coefficient (K_v) calculation

Parameters	TVIS
Drying rate at steady state (g/h) (2-2.8 h into primary drying)	0.42
Shelf Temperature, T_s (K)	273.3
Vial's base Temperature, T_b (K)	243.3

Objective

X

Heat transfer coefficient (K_v) calculation

Parameters	TVIS
Drying rate at steady state (g/h) (2-2.8 h into primary drying)	0.42
Shelf Temperature, T_s (K)	273.3
Vial's base Temperature, T_b (K)	243.3

$$L \frac{\Delta m}{\Delta t} = A_e K_v (T_s - T_b) \quad \Rightarrow$$

$$K_v = \frac{L \frac{\Delta m}{\Delta t}}{A_e (T_s - T_b)}$$

L is the latent heat of sublimation of ice ($2844 \text{ J}\cdot\text{g}^{-1}$ or $679.7 \text{ cal}\cdot\text{g}^{-1}$) and A_e is external cross-sectional area of the base of the TVIS vial (4.62 cm^2)

Objective X Heat transfer coefficient (K_v) calculation

Parameters	TVIS
Drying rate at steady state (g/h) (2-2.8 h into primary drying)	0.42
Shelf Temperature, T_s (K)	273.3
Vial's base Temperature, T_b (K)	243.3

$$L \frac{\Delta m}{\Delta t} = A_e K_v (T_s - T_b) \Rightarrow$$

$$K_v = \frac{L \frac{\Delta m}{\Delta t}}{A_e (T_s - T_b)}$$

L is the latent heat of sublimation of ice (2844 J·g⁻¹ or 679.7 cal·g⁻¹) and A_e is external cross-sectional area of the base of the TVIS vial (4.62 cm²)

$$K_v(270 \mu\text{bar}) = \frac{L \frac{\Delta m}{\Delta t}}{A_e (T_s - T_b)}$$

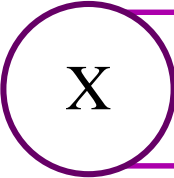
$$= \frac{679.7 \text{ cal} \cdot \text{g}^{-1} \times 0.42 \text{ g} \cdot \text{h}^{-1}}{4.62 \text{ cm}^2 \times (273.3 - 243.3) \text{ K}}$$

$$= 2.06 \text{ cal} \cdot \text{h}^{-1} \cdot \text{cm}^{-2} \cdot \text{K}^{-1}$$

$$= 5.73 \times 10^{-4} \text{ cal} \cdot \text{s}^{-1} \cdot \text{cm}^{-2} \cdot \text{K}^{-1}$$

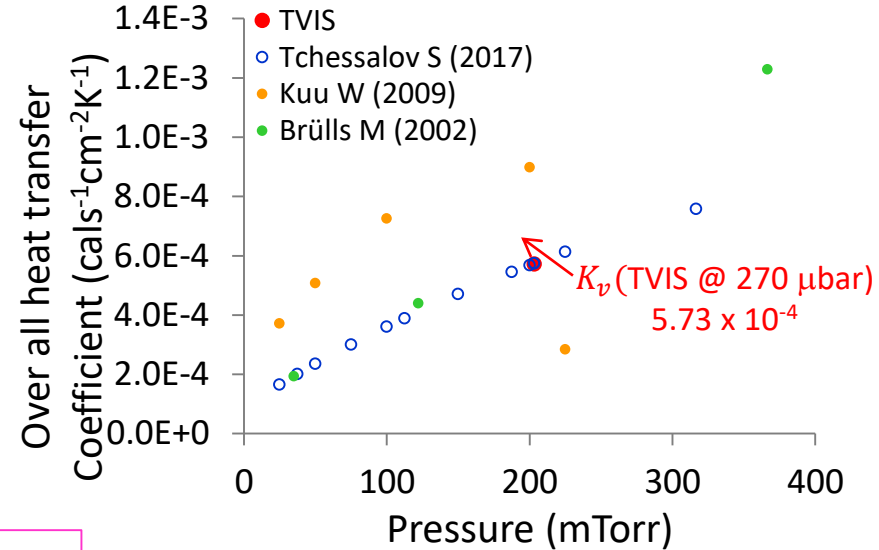
$$K_v(270 \mu\text{bar}) = 5.73 \times 10^{-4} \text{ cal} \cdot \text{s}^{-1} \cdot \text{cm}^{-2} \cdot \text{K}^{-1}$$

Objective



Heat transfer coefficient (K_v) calculation

Parameters	TVIS
Drying rate at steady state (g/h) (2-2.8 h into primary drying)	0.42
Shelf Temperature, T_s (K)	273.3
Vial's base Temperature, T_b (K)	243.3



$$L \frac{\Delta m}{\Delta t} = A_e K_v (T_s - T_b) \quad \Rightarrow$$

$$K_v = \frac{L \frac{\Delta m}{\Delta t}}{A_e (T_s - T_b)}$$

L is the latent heat of sublimation of ice ($2844 \text{ J}\cdot\text{g}^{-1}$ or $679.7 \text{ cal}\cdot\text{g}^{-1}$) and A_e is external cross-sectional area of the base of the TVIS vial (4.62 cm^2)

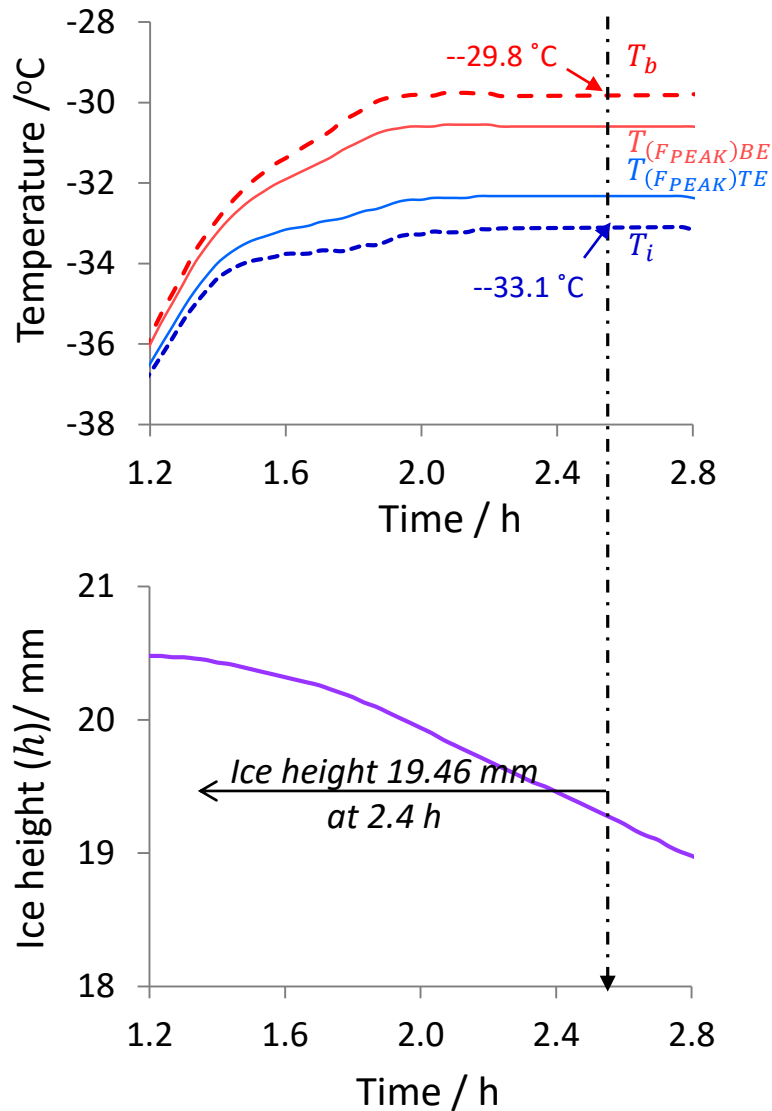
$$K_v(270 \mu\text{bar}) = \frac{L \frac{\Delta m}{\Delta t}}{A_e (T_s - T_b)}$$

$$\begin{aligned} &= \frac{679.7 \text{ cal}\cdot\text{g}^{-1} \times 0.42 \text{ g}\cdot\text{h}^{-1}}{4.62 \text{ cm}^2 \times (273.3 - 243.3)\text{K}} \\ &= 2.06 \text{ cal}\cdot\text{h}^{-1}\cdot\text{cm}^{-2}\cdot\text{K}^{-1} \\ &= 5.73 \times 10^{-4} \text{ cal}\cdot\text{s}^{-1}\cdot\text{cm}^{-2}\cdot\text{K}^{-1} \end{aligned}$$

$$K_v(270 \mu\text{bar}) = 5.73 \times 10^{-4} \text{ cal}\cdot\text{s}^{-1}\cdot\text{cm}^{-2}\cdot\text{K}^{-1}$$

Additional comments

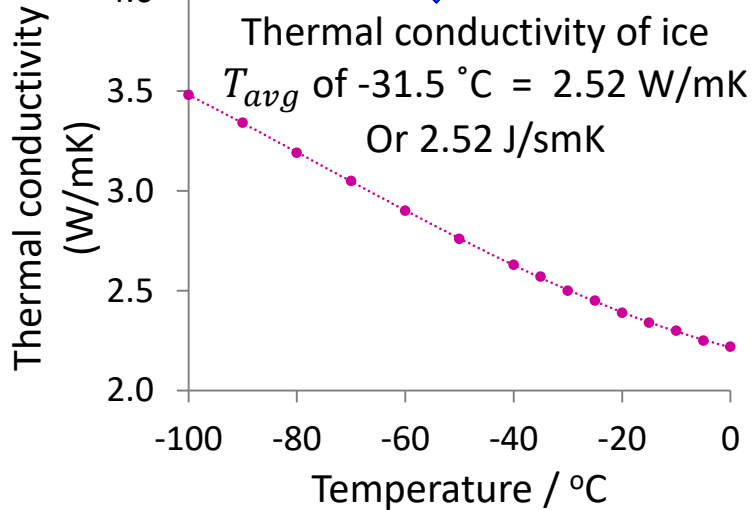
- 1) Calculation the relative heat transfer from the vial's base
- 2) Qualification of steady state heat transfer mechanisms



Parameters	TVIS
Ice interfacial temperature, T_i (K)	240.1
Vial's base Temperature, T_b (K)	243.3
Ice height or thickness of material, d (m)	0.0195
Average temperature (between T_i & T_b), T_{avg} ($^{\circ}\text{C}$)	-31.5
ΔT (between T_i & T_b) (K)	3.3

Objective

$$y = 4E-07x^3 + 0.0001x^2 - 0.0069x + 2.2174$$



Parameters	TVIS
Ice interfacial temperature, T_i (K)	240.1
Vial's base Temperature, T_b (K)	243.3
Ice height or thickness of material, d (m)	0.0195
Average temperature (between T_i & T_b), T_{avg} ($^{\circ}\text{C}$)	-31.5
ΔT (between T_i & T_b) (K)	3.3

$$\text{Drying rate } \left(\frac{\Delta m}{\Delta t}\right) = \frac{kA\Delta T}{Ld}$$



$$\frac{\Delta m}{\Delta t} = \frac{2.52\text{ W} \cdot \text{m}^{-1}\text{K}^{-1} \times 0.00038\text{ m}^2 \times 3.3\text{ K}}{2844 \times 0.0195}$$

$$= \frac{2.52\text{ J} \cdot \text{s}^{-1}\text{m}^{-1}\text{K}^{-1} \times 0.00038\text{ m}^2 \times 3.3\text{ K}}{2844\text{ J} \cdot \text{g}^{-1} \times 0.0195\text{ m}}$$

$$= 5.74 \times 10^{-5}\text{ g/s}$$

$$= \mathbf{0.207\text{ g/h}}$$



This drying rate is 50% of drying rate calculated by TVIS

k is the thermal conductivity constant for the material
 A is the cross sectional area of the material transferring heat (\equiv internal cross-sectional area of vial) 0.00038 m^2
 ΔT is the difference in temperature between one side of the material and the other
 L is Latent heat of sublimation at 240 K (2844 J/g)
 d is the thickness of the material (\equiv ice height)

A single vial technique

Pikal, et al. (1984)

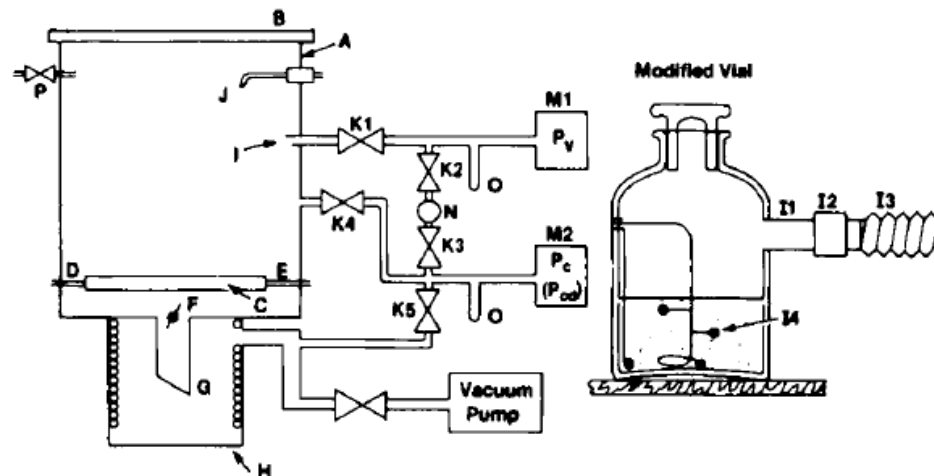


Figure 1—Schematic of the laboratory freeze-dryer (see text for key).

The mean sublimation rate was calculated from the mass of ice sublimed and the time required for sublimation.

Table IV—Evaluation of Heat Transfer by Top Radiation: Effective Emissivity, e_v

Product	N	A_v	$e_v \pm \sigma_m$
H ₂ O	7	4.71	0.83 ± 0.04
H ₂ O	3	6.83	0.94 ± 0.02
H ₂ O	3	17.2	0.79 ± 0.03
KCl ($I = 0$)	2	4.71	0.88
KCl ($I = 0.3$)	1	4.71	0.97
KCl ($I = 0$)	1	20.8	0.58
KCl ($I = 0.2$)	1	20.8	0.80
Mean			0.84

currred such that ice near the vial wall and ice near the thermocouple wire was preferentially removed. As a result of this phenomenon, measurements of temperature distribution in the ice had to be completed early in the experiment, before the assumption of a planar ice-vapor interface was seriously violated. Accurate temperature distribution data was obtained until ~15% of the ice had been removed. The vial heat transfer coefficient is defined assuming the ice at the vial bottom is in good thermal contact with the glass. Normally, with vials filled with pure water, partial loss of thermal contact occurs after sublimation of 35–50% of the ice. Thus, duration of a heat transfer experiment is limited to a time corresponding to sublimation of ~25% of the ice. Loss of thermal contact is rarely a problem when a frozen solution is dried.

For single vial heat transfer studies, a representative vial from a given lot of vials was modified as shown in Fig. 1. After filling, normally with pure water, the modified vial and other vials of the same lot, all equipped with "identical" metal tubes, were loaded into the laboratory dryer, the liquid was frozen, and the chamber was evacuated. The procedure then involved a series of heat transfer measurements under steady-state conditions at selected shelf temperatures and chamber pressures. An operational definition of steady state is taken as constant temperatures ($\pm 0.2^\circ\text{C}$) and pressures ($\pm 2 \mu\text{m}$) for a period of 10–15 min. The sublimation rate, \dot{m}_i , is calculated from the observed steady-state pressure readings using Eq. 3 with the closure resistance given by the tube resistance, Eq. 17. The heat transfer rate, \dot{Q} , is then calculated:

$$\dot{Q} \text{ (cal/s)} = 0.1833\dot{m} \text{ (g/h)} \quad (\text{Eq. 18})$$

A single vial technique

Scutella, et al. 2017

Ice Sublimation Experiments

All experiments were performed using a 1.8-mL fill volume of distilled water (filling height: 11 mm). No stopper was inserted into the vial neck. The middle shelf was fully covered by filled vials for all runs, corresponding to a total of 540 vials in LYO A and 950 vials in LYO B. Bottomless trays were used.

The vials were quickly loaded on the pre-cooled shelf at -50°C . The presence of a dry laminar flow in front of the freeze-dryer door made it possible to control the air relative humidity and thus to limit condensation on the shelves. After a freezing step of 2 h, the pressure was decreased and the shelf temperature was increased by $1^{\circ}\text{C}/\text{min}$. Experiments were carried out at 4, 6, 9, 15, 40, and 50 Pa with a shelf fluid inlet temperature of 0°C , and at 4 and 6 Pa with a shelf fluid inlet temperature of -40°C . The run performed at 0°C and 6 Pa was repeated 3 times. **The cycles were run long enough to dry up to 20%-25% of the initial fill volume. Subliming a larger quantity of ice could lead to loss of contact between the vial and the ice, introducing uncertainty in the analysis.**

The sublimation rate \dot{m} was measured gravimetrically for each vial and calculated as the mass loss divided by the period of sublimation. A total of 100 vials, placed in the center of the shelf and surrounded by other vials in the same conditions, were individually weighed before and after the experiment on a precision scale (± 0.001 g; Mettler Toledo, Zaventem, Belgium). Sublimation time was measured from the moment when shelf fluid inlet temperature exceeded product temperature, meaning that there was a net heat flux from the shelf toward the vials. The

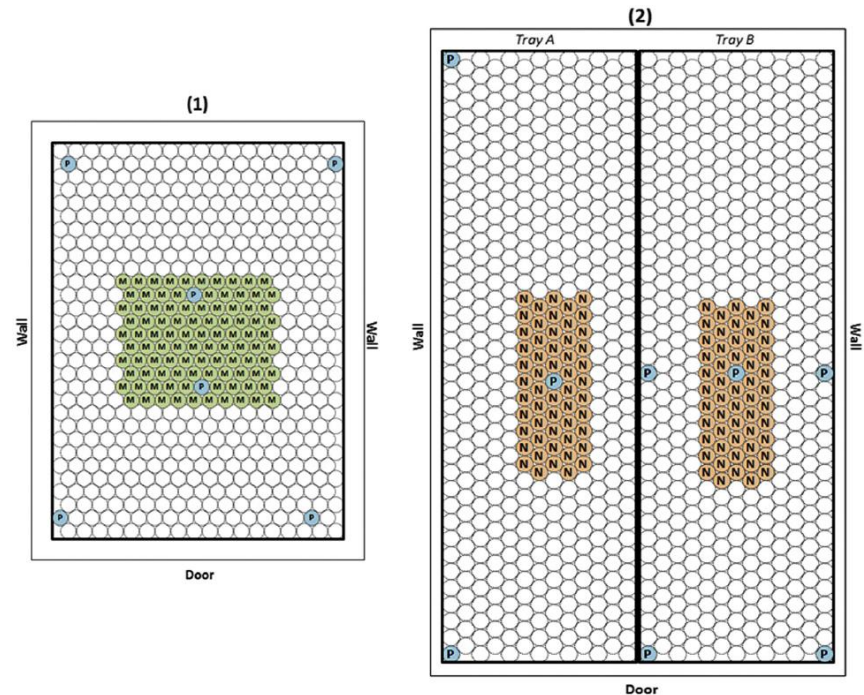
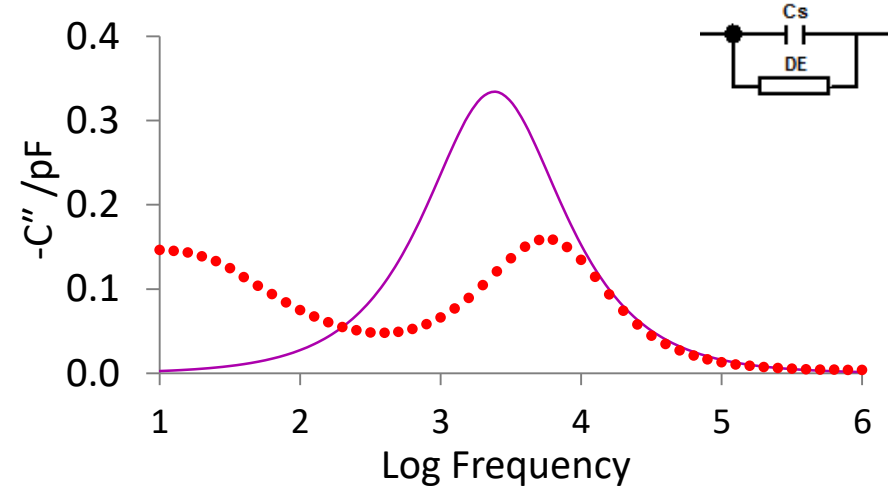
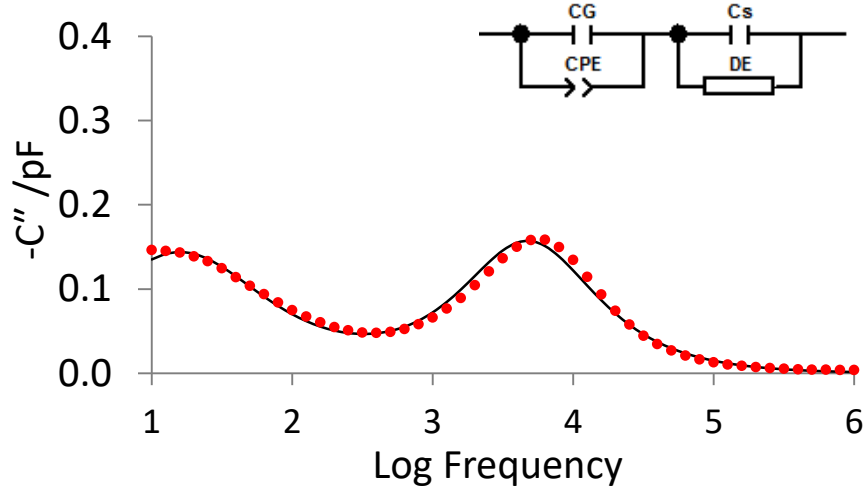


Figure 1. Vial arrangements in (1) LYO A and (2) LYO B. Gravimetrically analyzed vials are marked with the letters M and N for LYO A and B, respectively. Vials in which wireless temperature probes were located are marked with the letter P. All vials were filled with 1.8 mL of pure water.

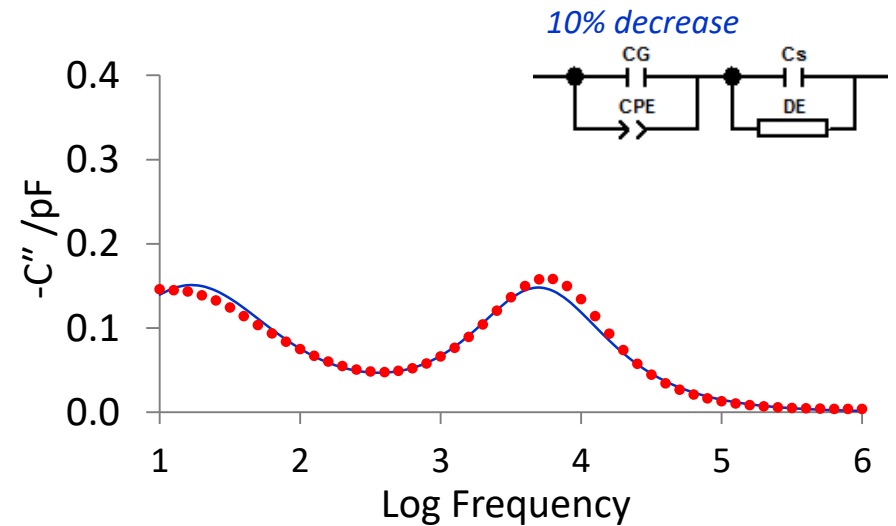
Assumption for K_v determination

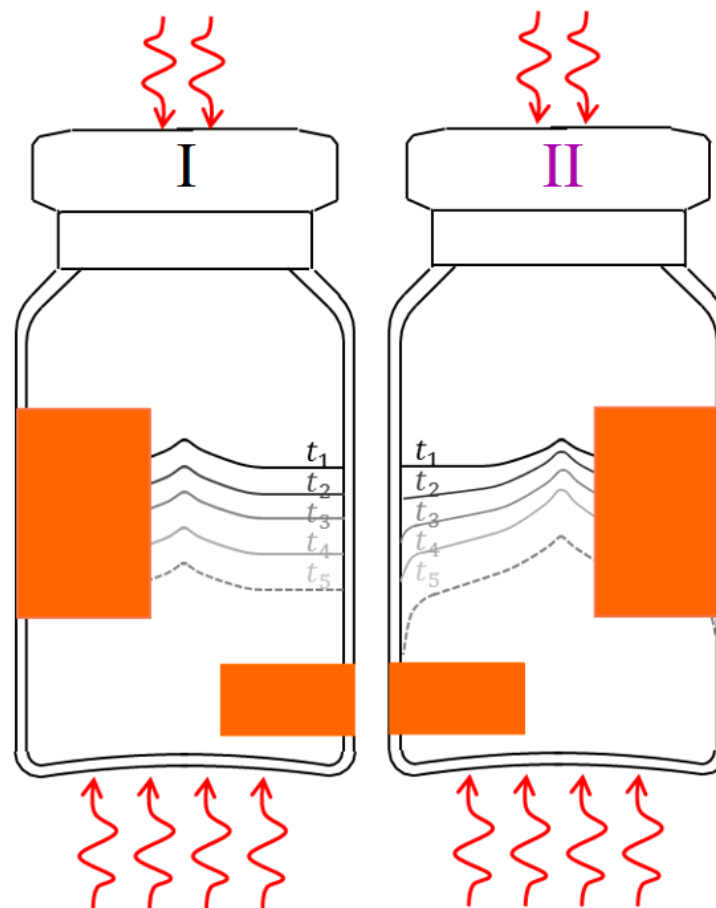
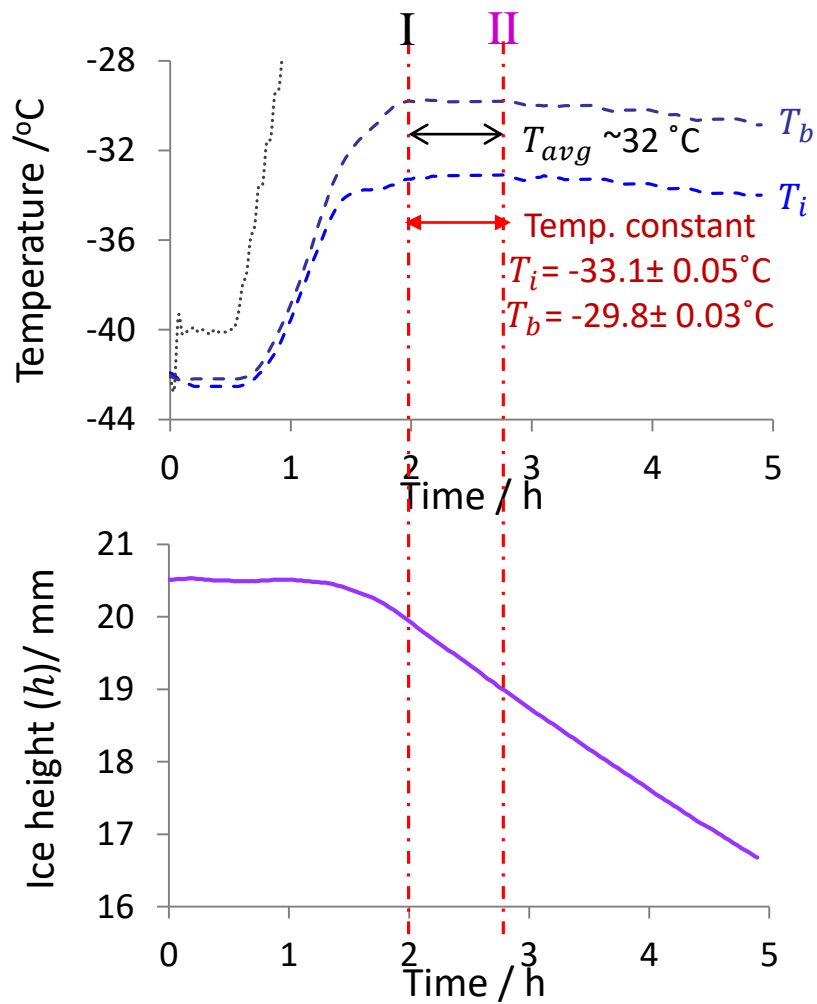
- How do we know the heat transfer mechanisms constant up to 25% loss of ice mass?
- If the heat transfer mechanisms change because of ice- glass interface contact or because of the change of ice shape (surface area), then surely heat transfer coefficient will change.
- It requires the technique to qualify when the heat transfer mechanisms change

Limitation of TVIS Systems



- Glass wall impedance can increase the peak frequency (F_{PEAK}) but reduce the peak amplitude (C''_{PEAK})
- Decrease in F_{PEAK} during primary drying is due to loss of contact of ice with the side wall





Discussion

- Decrease in F_{PEAK} suggests that the temperature may be decreasing after the steady state period, contrary to accepted knowledge that the temperature starts to increase owing to a reduction in drying rate and hence the degree of self cooling
- Decrease in F_{PEAK} is more likely to be due to a change in the ice-glass contact associated with a change in the shape of the ice cylinder.

Conclusion

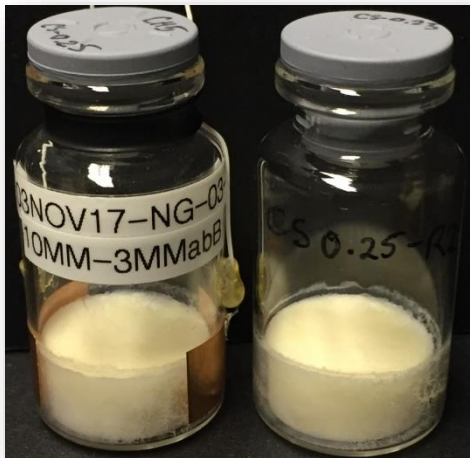
- The period for determining the drying rate should be decreased from 25% ice loss to 10% suggested by our experiment.

Limitations

- C''_{PEAK} and F_{PEAK} parameters rely on intimate contact of ice cylinder with glass wall
- $C'(100\text{ kHz})$ parameter does not depend on contact and can be used for end point but relationship between $C'(100\text{ kHz})$ ice constant is non-linear
- Cable length limited to 1m at present
- C-TVIS not compatible with front loading system
- Incompatible with TCs in same TVIS vial (use fibre optic sensors – INFAP)

Future Work

- Development mapping a drying characteristics
 - heat transfer coefficients (K_V)
 - dry layer resistance (R_P)



- Instrument Development
 - Commercial C-TVIS (2018)
 - Non-contact TVIS (2018-19)
 - Micro-well screening
 - Vial clusters in batch FD
 - TVIS - Shuttle (2019-20)

Non-invasive real time information for characterising the freeze drying

Acknowledgements, Recent Projects & Collaborators

- De Montfort University, School of Pharmacy
 - Evgeny Polygalov: co-inventor of TVIS instrument
 - Yowwares Jeeraruangrattana. PhD student
 - Bhaskar Pandya. PhD student
 - Irina Ermolina. Senior Lecturer



Through Vial Impedance Spectroscopy



Acknowledgements, Recent Projects & Collaborators

- De Montfort University
 - Evgeny Polygalov. Senior Research Fellow
 - Irina Ermolina. Senior Lecturer
 - Yowwares Jeerarunangrattana. PhD student
 - Bhaskar Pandya. PhD student
- GEA Process Engineering
 - Trevor Page & Julian Taylor
 - Daniela Buchmeyer & Thomas Beutler
- BlueFrog : Chris Samwell Ben Irvin
- NIBSC : Paul Matejtschuk
- Sanofi : Tim McCoy



GEA Pharma Systems



Innovate UK

Thank you

Objective

I

TVIS temperature calibration of $\log F_{PEAK}$ of top electrode ($T_{(F_{PEAK})TE}$) and bottom electrode ($T_{(F_{PEAK})BE}$)



Objective

II

Calibration C''_{PEAK} by accounting for the temperature dependency of C''_{PEAK}



Objective

III

Development method for temperature compensation of C''_{PEAK} during primary drying



Objective

IV

Prediction of ice temperatures at (i) interface (T_i) and (ii) base (T_b) including qualification TVIS technique ($T_i = T_{(P_i=P_c)}$)



Objective

V

Estimation the surrogate drying rate ($\Delta m/\Delta t$) and evaluation TVIS determination with gravimetric method (weight loss)

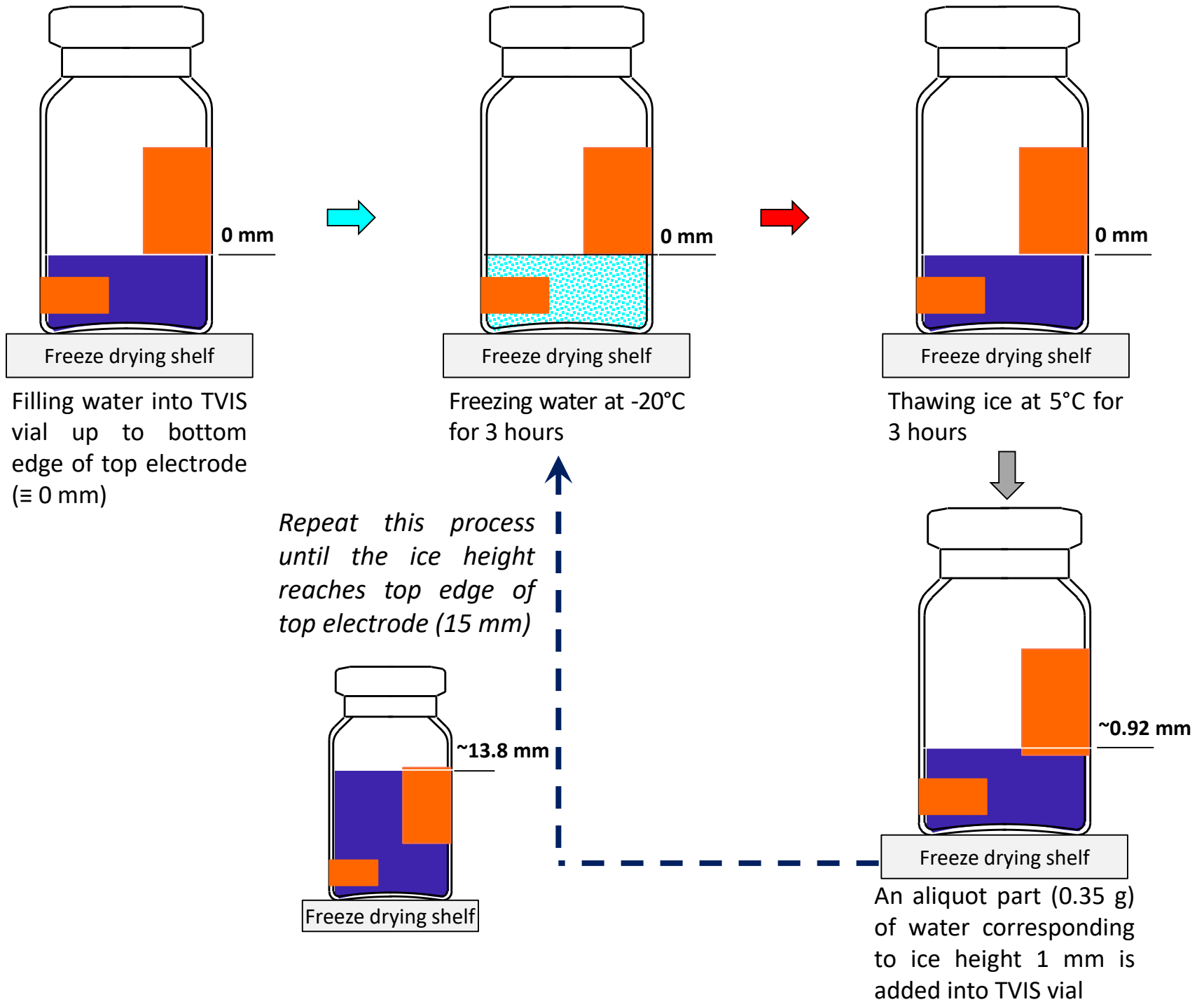


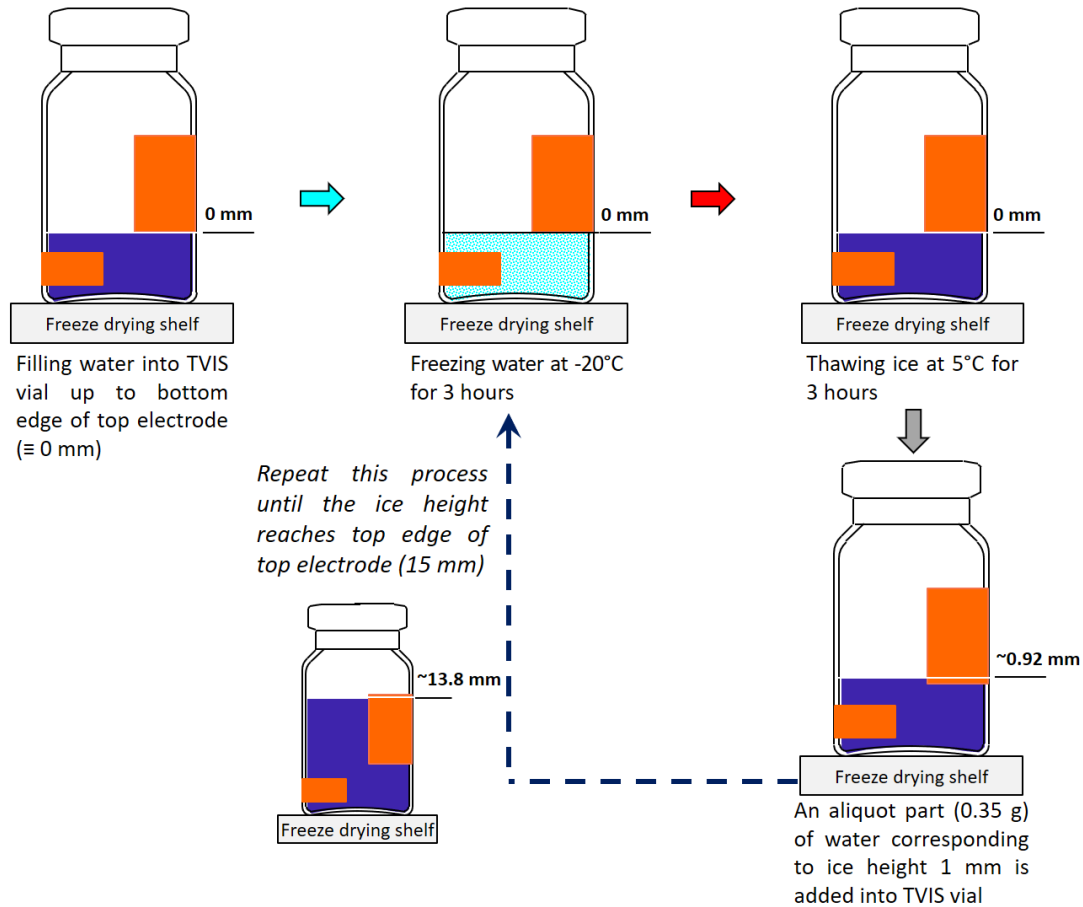
Objective

VI

Determination (i) the drying rate ($\Delta m/\Delta t$) and (ii) ice base temperature (T_b) during the steady state period for heat transfer coefficient (K_v) calculation



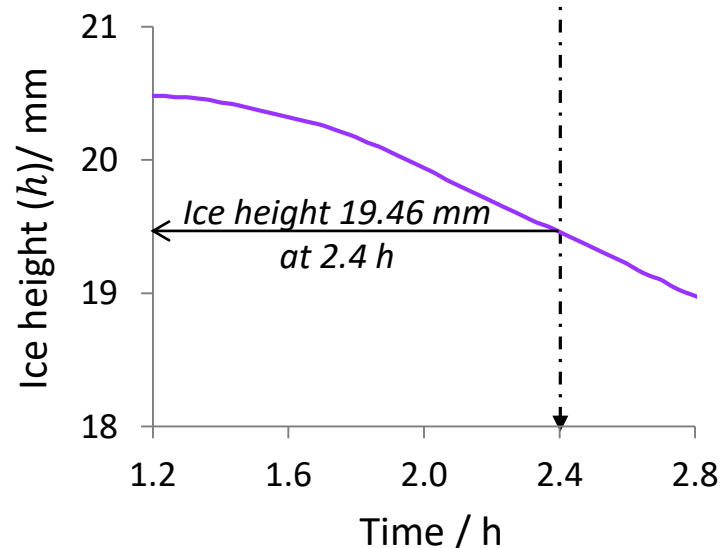
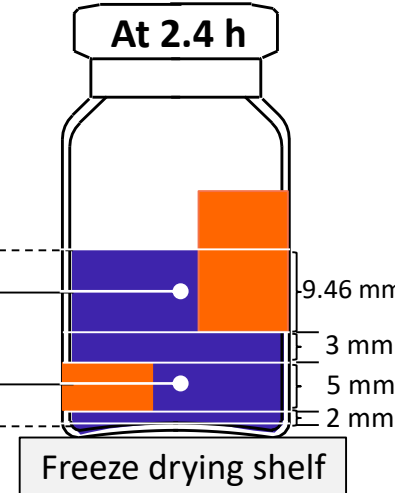
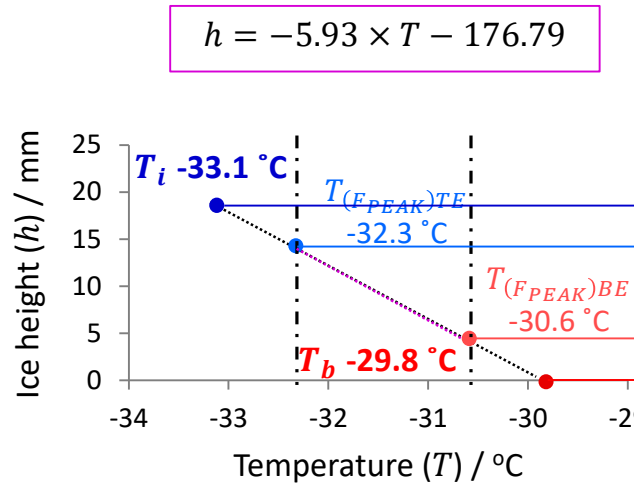
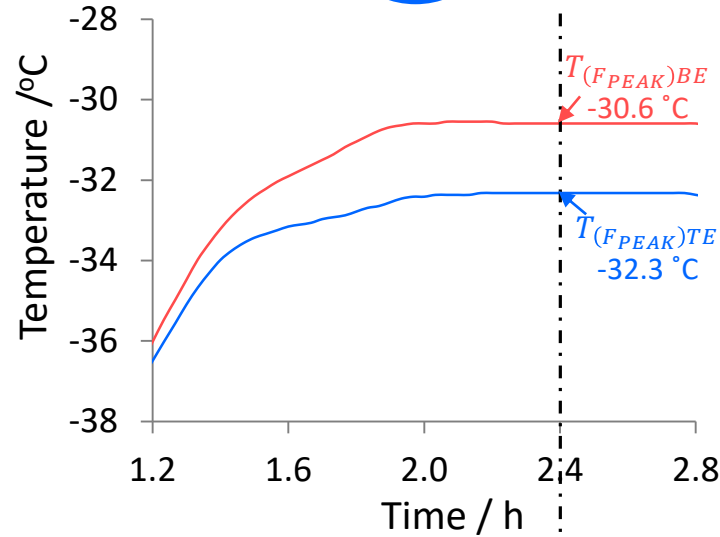




Objective

VII

Prediction ice temperatures at (i) sublimation interface (T_i) and (ii) vial's base (T_b) including qualification TVIS technique ($T_i = T_{(P_i=P_c)}$)



Ice height for $T_{(F_{PEAK})TE}$ = $2 + 5 + 3 + \left(\frac{9.46}{2}\right) = 14.73\text{ mm}$

Ice height for $T_{(F_{PEAK})BE}$ = $2 + \left(\frac{5}{2}\right) = 4.50\text{ mm}$

$h = -5.93 \times T - 176.79$ \Rightarrow $T = \frac{h + 176.79}{-5.93}$

Ice Temperature

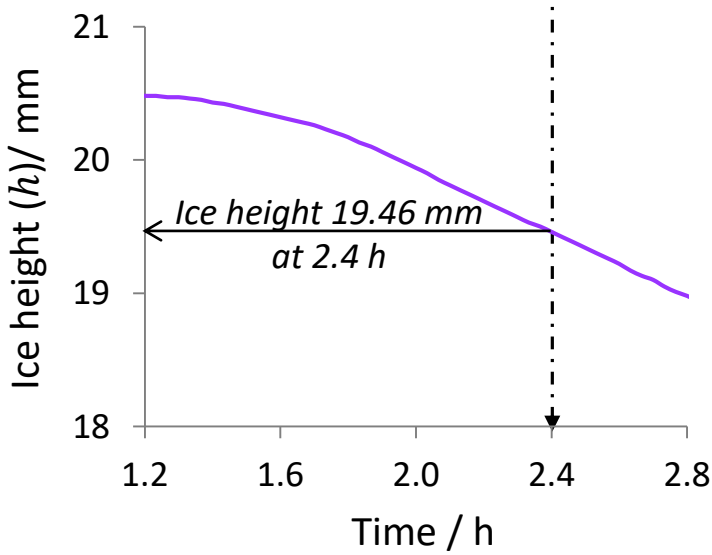
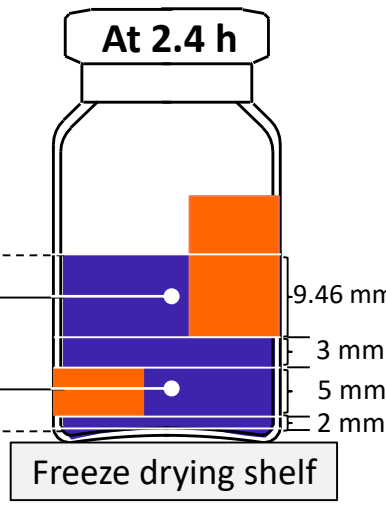
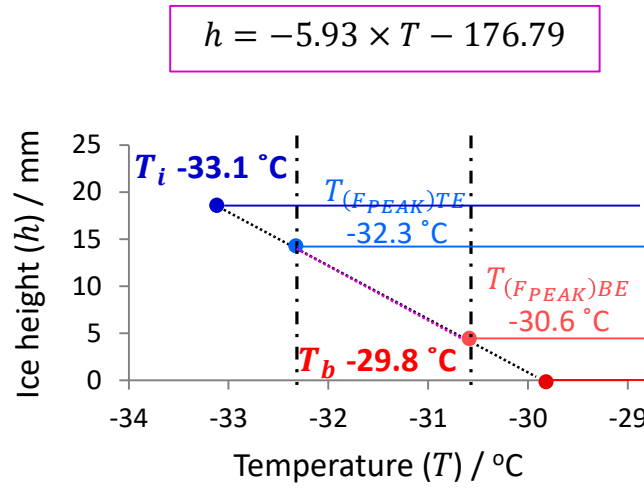
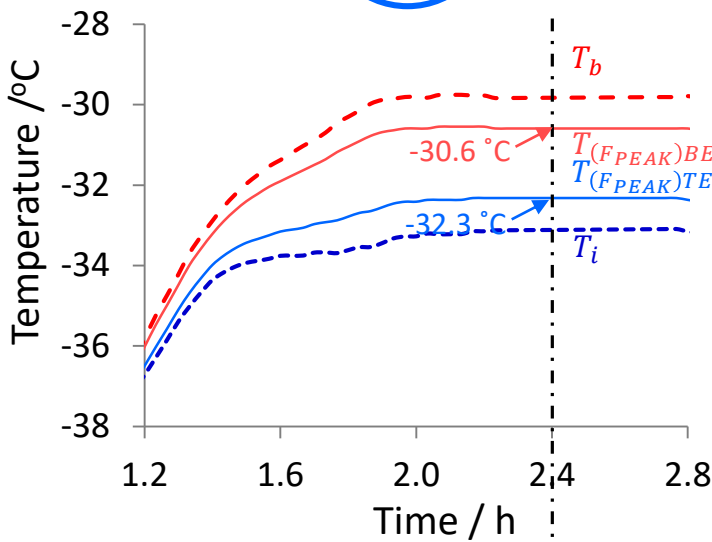
At interface ($T_i, 19.46\text{ mm}$) = $\frac{h+176.79}{-5.93} = \frac{19.46+176.79}{-5.93} = -33.1\text{ °C}$

At vial's base ($T_b, 0\text{ mm}$) = $\frac{h+176.79}{-5.93} = \frac{0+176.79}{-5.93} = -29.8\text{ °C}$

Objective

VII

Prediction ice temperatures at (i) sublimation interface (T_i) and (ii) vial's base (T_b) including qualification TVIS technique ($T_i = T_{(P_i=P_c)}$)



Ice height for $T_{(FPEAK)TE}$ = $2 + 5 + 3 + \left(\frac{9.46}{2}\right) = 14.73$ mm

Ice height for $T_{(FPEAK)BE}$ = $2 + \left(\frac{5}{2}\right) = 4.50$ mm

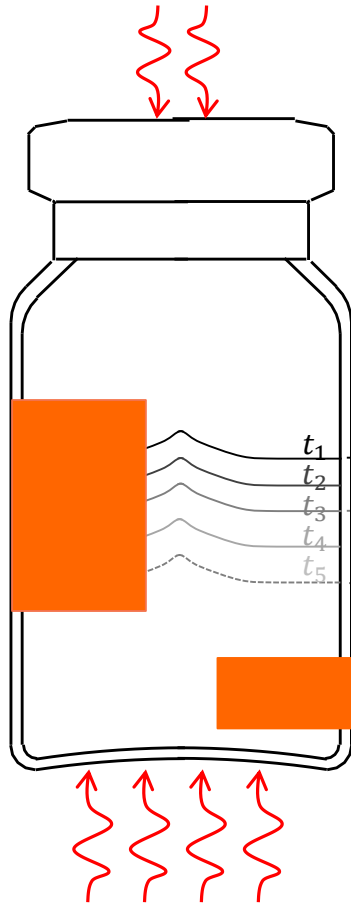
$h = -5.93 \times T - 176.79$ \Rightarrow $T = \frac{h + 176.79}{-5.93}$

Ice Temperature

At interface ($T_i, 19.46$ mm) = $\frac{h+176.79}{-5.93} = \frac{19.46+176.79}{-5.93} = -33.1$ °C

At vial's base ($T_b, 0$ mm) = $\frac{h+176.79}{-5.93} = \frac{0+176.79}{-5.93} = -29.8$ °C

Ice Cylinder in Contact with the Inside of the Glass Wall

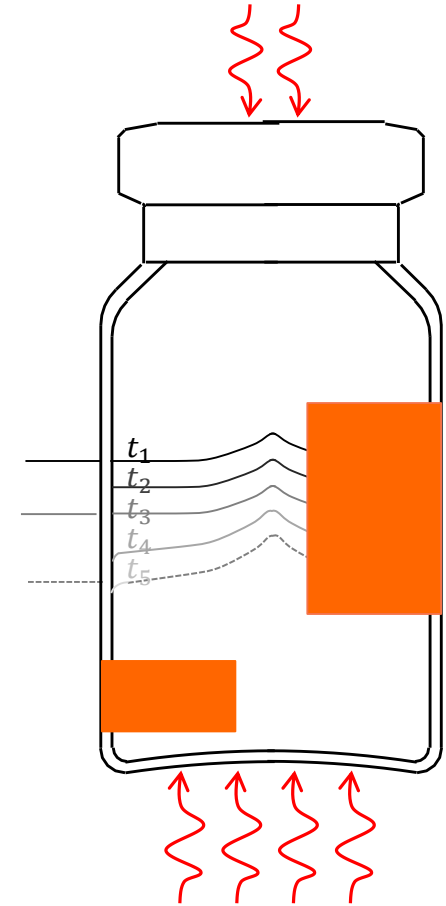


1

10.5 mm. from bottom edge of electrode ($\varnothing = 0.7$)

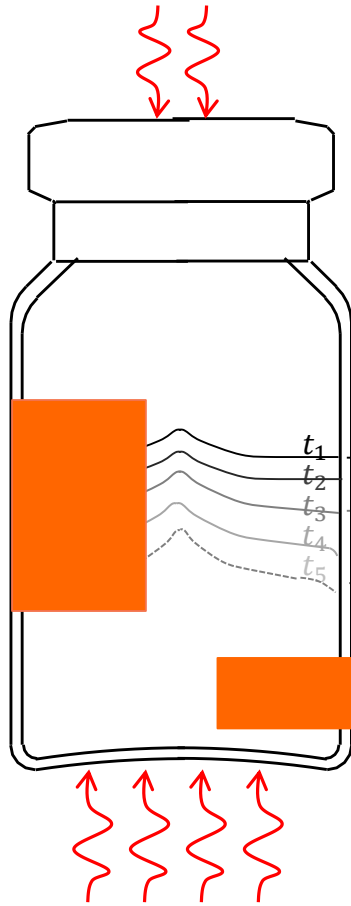
25% of ice has been removed ($\varnothing = 0.53$)

2 mm. from bottom edge of electrode ($\varnothing = 0.13$)



2

Ice Cylinder in Contact with the Inside of the Glass Wall

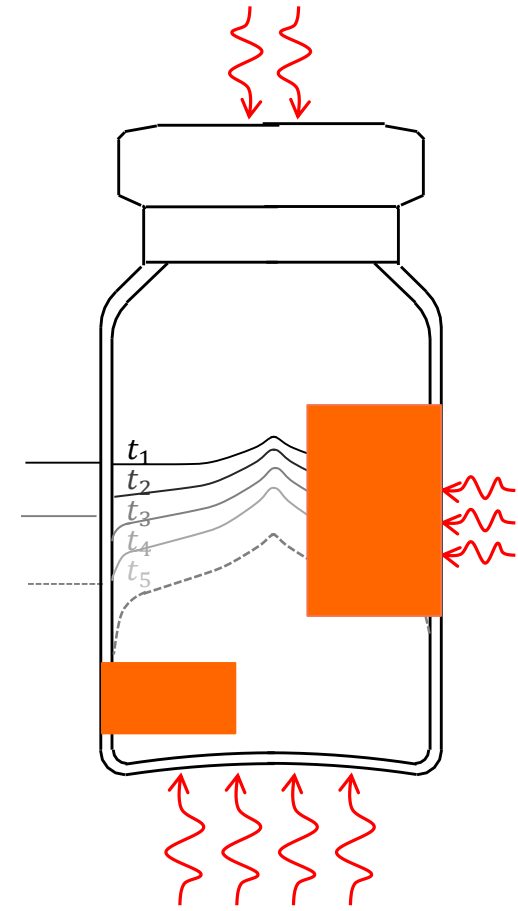


3

10.5 mm. from bottom edge of electrode ($\phi = 0.7$)

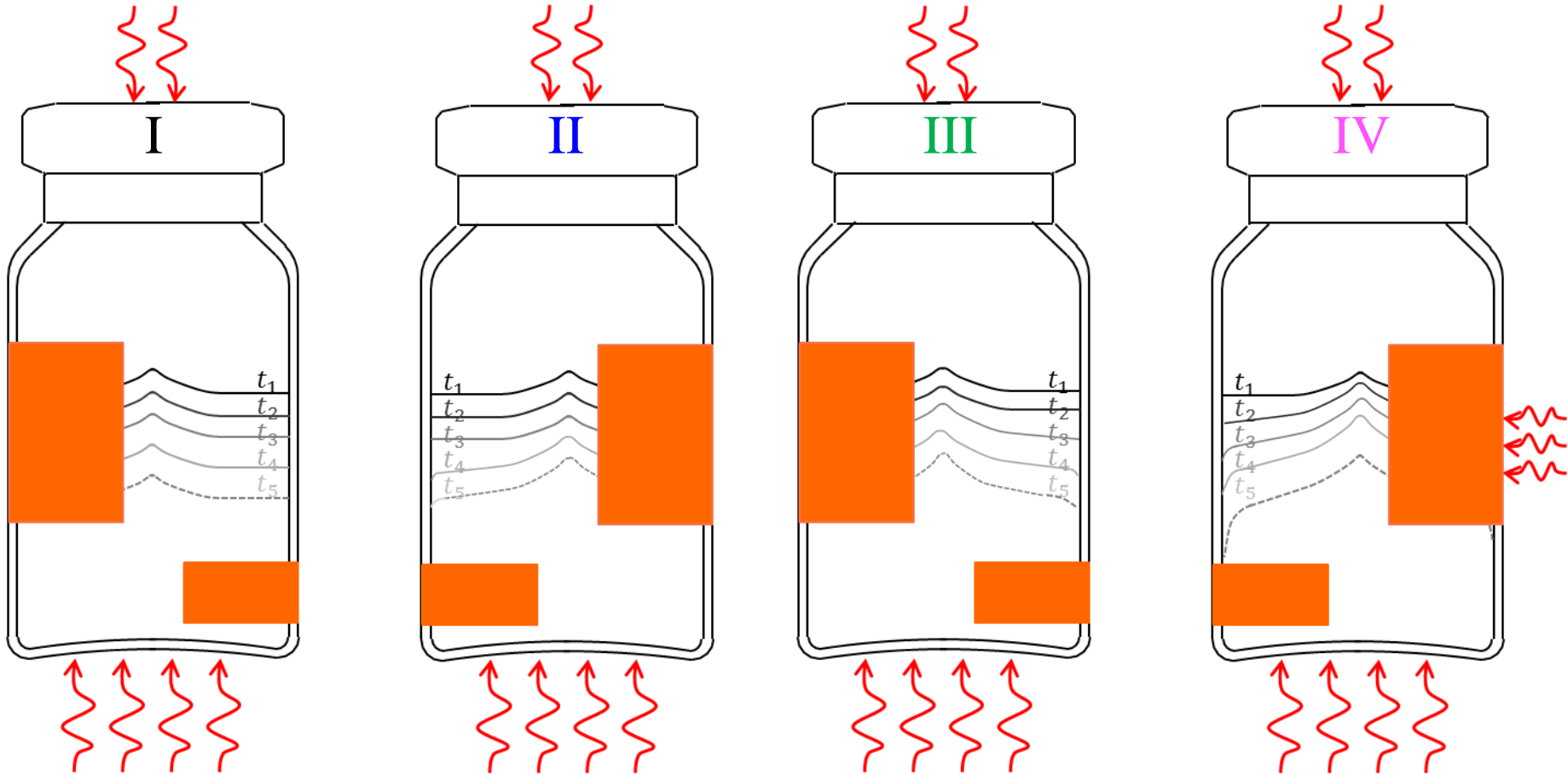
25% of ice has been removed ($\phi = 0.53$)

2 mm. from bottom edge of electrode ($\phi = 0.13$)



4

Ice Cylinder in Contact with the Inside of the Glass Wall



Ice Cylinder in Contact with the Inside of the Glass Wall

